

1 **A chromosome-level assembly of the black tiger shrimp (*Penaeus monodon*) genome facilitates
2 the identification of novel growth-associated genes**

3

4 Tanaporn Uengwetwanit^{1,†}, Wirulda Pootakham^{2,†}, Intawat Nookaew³, Chutima Sonthirod²,
5 Pacharaporn Angthong¹, Kanchana Sittikankaew¹, Wanilada Rungrassamee¹, Sopacha
6 Arayamethakorn¹, Thidathip Wongsurawat³, Piroon Jenjaroenpun³, Duangjai Sangsrakru², Rungnapa
7 Leelatanawit¹, Jutatip Khudet⁴, Jasper J. Koehorst⁵, Peter J. Schaap⁵, Vitor Martins dos Santos⁵,
8 Frédéric Tangy⁶, Nitsara Karoonuthaisiri^{1,*}

9

10 ¹National Center for Genetic Engineering and Biotechnology (BIOTEC), National Science and
11 Technology Development Agency, Pathum Thani, 12120, Thailand

12 ²National Omics Center, National Center for Genetic Engineering and Biotechnology (BIOTEC),
13 National Science and Technology Development Agency, Pathum Thani, 12120, Thailand

14 ³Department of Biomedical Informatics, College of Medicine, University of Arkansas for Medical
15 Sciences, Little Rock, Arkansas, 72205, USA

16 ⁴Shrimp Genetic Improvement Center, Integrative Aquaculture Biotechnology Research Group, Surat
17 Thani, 84110, Thailand

18 ⁵Laboratory of Systems and Synthetic Biology, Department of Agrotechnology and Food Sciences,
19 Wageningen University and Research, 6708WE Wageningen, Netherland

20 ⁶Viral Genomics and Vaccination Unit, UMR3569 CNRS, Virology department, Institut Pasteur,
21 75015, Paris, France

22

23 [†]These authors contributed equally to this work

24 *Correspondence should be addressed to NK (nitsara@alumni.stanford.edu)

25

26 **Abstract**

27 The black tiger shrimp (*Penaeus monodon*) is one of the most prominent farmed crustacean species
28 with an average annual global production of 0.5 million tons in the last decade. To ensure sustainable
29 and profitable production through genetic selective breeding programs, several research groups have
30 attempted to generate a reference genome using short-read sequencing technology. However, the
31 currently available assemblies lack the contiguity and completeness required for accurate genome
32 annotation due to the highly repetitive nature of the genome and technical difficulty in extracting high-
33 quality, high-molecular weight DNA in this species. Here, we report the first chromosome-level
34 whole-genome assembly of *P. monodon*. The combination of long-read Pacific Biosciences (PacBio)
35 and long-range Chicago and Hi-C technologies enabled a successful assembly of this first high-quality
36 genome sequence. The final assembly covered 2.39 Gb (92.3% of the estimated genome size) and
37 contained 44 pseudomolecules, corresponding to the haploid chromosome number. Repetitive
38 elements occupied a substantial portion of the assembly (62.5%), highest of the figures reported
39 among crustacean species. The availability of this high-quality genome assembly enabled the
40 identification of novel genes associated with rapid growth in the black tiger shrimp through the
41 comparison of hepatopancreas transcriptome of slow-growing and fast-growing shrimps. The results
42 highlighted several gene groups involved in nutrient metabolism pathways and revealed 67 newly
43 identified growth-associated genes. Our high-quality genome assembly provides an invaluable
44 resource for accelerating the development of improved shrimp strain in breeding programs and future
45 studies on gene regulations and comparative genomics.

46

47 **Keywords**

48 Black tiger shrimp; *Penaeus monodon*; reference genome; Hi-C; PacBio; growth-associated
49 genes; transcriptomics

50

51 **Introduction**

52 Aquaculture is an important food source for the world's growing population as it relieves the
53 over-consumption pressure of natural animal populations within the aquatic environment. Currently,
54 aquaculture provides the planet with more than 50 percent of fish products consumed by humans,
55 making it one of the world's fastest-growing food sectors with an annual growth rate of 5.8 percent
56 since 2010 (FAO, 2018). The penaeid marine shrimps (Family Penaeidae) are the predominately
57 cultured group (Thornber et al., 2019), with an annual production exceeding 4.5 million tons
58 (Anderson, 2019). In this group, the Pacific white shrimp (*Litopenaeus vannamei*) and black tiger
59 shrimp (*Penaeus monodon*) are the most dominant species cultured, accounting for 53% and 9% of
60 total crustacean production, respectively (FAO, 2018).

61 While the penaeid industry has seen dramatic growth for the past few decades, industrial
62 production of *P. monodon* proved to be unsustainable due to a lack of biological and genetic
63 knowledge to achieve its desirable traits such as fast growth, disease resistance, reproductive
64 maturation without reliance on wild brooders (Guppy et al., 2018). Recently, the *L. vannamei* breeding
65 and domestication programs can be expeditedly improved due to the available genome sequence, which
66 allows selective breeding and helps in overcoming industrial challenges (Zhang et al., 2019).
67 Genomic-driven breeding and domestication programs for *P. monodon*, on the other hand, are still in
68 their infancy due to the absence of an informative high-quality draft genome sequence.

69 While such a high-quality draft genome sequence has not been reported for *P. monodon*, several
70 efforts have been made to investigate the genome and genetic architecture of this important species
71 over the past few decades. BAC library construction (Wuthisuthimethavee, Aoki, Hirono, &
72 Tassanakajon, 2009), fosmid library end sequencing (Huang et al., 2011), molecular marker
73 development (Brooker, Benzie, Blair, & Versini, 2000; A. Tassanakajon, Pongsomboon, Jarayabhand, &
74 Klinbunga, & Boonsaeng, 1998; A. Tassanakajon, Pongsomboon, Rimphanitchayakit, Jarayabhand, &
75 Boonsaeng, 1997), linkage map construction (Baranski et al., 2014; Wilson et al., 2002), and
76 transcriptomic analysis (Karoonuthaisiri et al., 2009; Leelatanawit, Uawisetwathana, Klinbunga, &
77 Karoonuthaisiri, 2011; Lehnert, Wilson, Byrne, & Moore, 1999; Pootakham, Uengwetwanit,

78 Sonthirod, Sittikankaew, & Karoonuthaisiri, 2020; Sittikankaew et al., 2020; Supungul et al., 2002;
79 Anchalee Tassanakajon et al., 2006; Tong, Lehnert, Byrne, Kwan, & Chu, 2002; Uengwetwanit et al.,
80 2018; Wongsurawat et al., 2010) were explored with limited success. Previous attempts to obtain
81 genome sequences in the black tiger shrimp relied primarily on short-read sequencing platforms due to
82 cost and technical difficulty in extracting high-quality, high-molecular weight DNA in this species
83 (Quyen et al., 2020; Yuan et al., 2018). Recently, two draft genomes for *P. monodon* were made
84 available; however, both versions of the assemblies were highly fragmented, with N50 contig lengths
85 of merely 937 nt (Yuan et al., 2018) and 1,982 nt (Quyen et al., 2020). Even though those resources
86 were useful for the black tiger shrimp genetics, they lacked the contiguity and completeness required
87 for accurate genome annotation and thorough comparative genomics analyses.

88 Here, we combined a long-read sequencing technology and two long-range scaffolding
89 techniques to obtain high-quality, chromosome-scale genome assembly. First, the Pacific Biosciences
90 (PacBio) sequencing platform was employed to generate the preliminary assembly. The PacBio
91 sequencing technology enables contiguous assembly of repetitive regions containing transposable
92 elements and tandem repeats, which are often omitted or highly fragmented in genomic sequences
93 currently available in public databases. We subsequently applied the long-range Chicago (*in vitro*
94 proximity ligation) and Hi-C (*in vivo* fixation of chromosomes) scaffolding techniques to further
95 scaffold the preliminary assembly to achieve the first chromosome-scale genome assembly in *P.*
96 *monodon*. The utility of this dramatically improved assembly in elucidating novel genes involved in
97 growth regulation was demonstrated by the transcriptome analysis of slow-growing and fast-growing
98 black tiger shrimps. Our high-quality, chromosome-scale genome assembly provides a valuable
99 genetic resource for black tiger shrimp breeding programs and future gene expression and comparative
100 genomics studies in this species.

101

102 **Materials and Methods**

103 **Sample collection and DNA extraction**

104 The muscle of a 5-month-old female *P. monodon* was collected from the Shrimp Genetic
105 Improvement Center (SGIC, Surat Thani, Thailand), immediately frozen in liquid nitrogen and stored
106 at -80 °C until use. Frozen muscle was pulverized in liquid nitrogen and genomic DNA was extracted
107 using a Genomic Tip 100/G kit (Qiagen, USA). DNA quantity was measured using a NanoDrop ND-
108 8000 spectrophotometer and a Qubit dsDNA BR Assay kit (Invitrogen, USA) using Qubit
109 fluorometer. The DNA quality and integrity were visualized under pulsed-field gel electrophoresis at
110 80 volts for 9 h in 0.5x KBB buffer (51 mM Tris, 28 mM TASP, 0.08 mM EDTA, pH 8.7) (Sage
111 Science, USA) containing SYBR Safe DNA gel staining (Invitrogen, USA).

112

113 **PacBio library preparation and sequencing**

114 Whole genome sequencing was performed using long read PacBio RS II and SEQUEL (Pacific
115 Biosciences, Menlo Park, USA, outsourced to NovogenAIT, Singapore). The 15-kb and 20-kb
116 SMRTbell libraries were constructed for the PacBio RSII and SEQUEL systems, respectively. For
117 short read sequencing, the paired-end library with 150 bp was prepared and sequenced Illumina HiSeq
118 2000 (Illumina, San Diego, USA) that was outsourced to Novogene, USA

119

120 **Illumina library preparation and sequencing**

121 The short paired-end library (2x150 bp) was sequenced on the Illumina instrument at
122 Novogene (USA). These illumine reads (133X coverage) were used to correct error reads of *de novo*
123 assembly.

124

125 **Chicago library preparation and sequencing**

126 A Chicago library was prepared as described previously (Putnam et al., 2016). Approximately,
127 500ng of high molecular weight genomicDNA (mean fragment length = 60 kbp) was reconstituted into
128 chromatin *in vitro* and fixed with formaldehyde. Fixed chromatin was digested with DpnII, the 5'
129 overhangs filled in with biotinylated nucleotides, and then free blunt ends were ligated. After ligation,

130 crosslinks were reversed to remove protein from DNA. Purified DNA was treated to remove biotin
131 that was not internal to ligated fragments. The DNA was then sheared to ~350 bp mean fragment size
132 and sequencing libraries were generated using NEBNext Ultra enzymes and Illumina-compatible
133 adapters. Biotin-containing fragments were isolated using streptavidin beads before PCR enrichment
134 of each library. The libraries were sequenced on an Illumina HiSeq X to produce 444 million 2x150 bp
135 paired end reads, which provided 51.89 x physical coverage of the genome (1-100 kb pairs).

136

137 **Dovetail Hi-C library preparation and sequencing**

138 A Dovetail Hi-C library was prepared in a similar way as described previously (Lieberman-
139 Aiden et al., 2009). For each library, chromatin was fixed in place with formaldehyde in the nucleus,
140 and then extracted fixed chromatin was digested with DpnII, the 5' overhangs filled in with
141 biotinylated nucleotides, and then free blunt ends were ligated. After ligation, crosslinks were reversed
142 to remove protein from DNA. The purified DNA were then processed as similar as aforementioned in
143 Chicago library preparation. The libraries were sequenced on an Illumina HiSeq X to produce 430
144 million 2x150 bp paired end reads, which provided 24,424.63X physical coverage of the genome (10-
145 10,000 kb pairs).

146

147 **Genome assembly and scaffolding**

148 Three types of sequencing reads from Illumina, PacBio, and Dovetail (Chicago and Hi-C reads)
149 were used to construct *P. monodon* genome. PacBio sequence data was used for *de novo* assembly and
150 Illumina sequence data was subsequently used for polishing to obtain high quality contigs. Chicago
151 and Hi-C reads were used for scaffolding on the high quality contigs to obtain high quality *P.*
152 *monodon* draft genome. In brief, high quality Illumina reads were prepared using TrimGalore
153 (<https://github.com/FelixKrueger/TrimGalore>) based on the following criteria: (i) no “N” base, (ii)
154 trimming of adaptor sequences and low quality bases (Q<20), (iii) no trimmed reads < 100 bp. To
155 avoid mis-assembly due to repetitive sequences (Tørresen et al., 2019), PacBio SEQUEL subreads

156 with repetitive sequences comprised over 85% of total sequences were filtered out. The GC content
157 criteria (<25% and >85%) was applied for filtering low complexity DNA sequences before assembly.
158 Noted that GC content of crustacean are 35-41% (Gao et al., 2017; Yu et al., 2015; Zhao et al., 2012).
159 Moreover, the reads matched mitochondria sequence (NC_002184.1) were excluded from nucleus
160 sequences and processed separately (Supplemental method). The reads \geq 5,000 bp were assembled
161 using WTDBG2 (Hu et al., 2019). Illumina reads were then aligned to the assembled contigs by
162 minimap2 (Li, 2018) and subjected for polishing using wtpoa-cns mode in WTDBG2 (Hu et al.,
163 2019).

164 Scaffolding of the genome assemblies was performed using HiRise, a software pipeline
165 designed specifically for using proximity ligation data to scaffold genome assemblies (Putnam et al.,
166 2016). The input *de novo* assembly, shotgun reads, Chicago library reads, and Dovetail Hi-C library
167 reads were used as input data for HiRise. An iterative analysis was conducted. First, shotgun and
168 Chicago library sequences were aligned to the draft input assembly using a modified SNAP read
169 mapper (<http://snap.cs.berkeley.edu>). The separations of Chicago read pairs mapped within draft
170 scaffolds were analyzed by HiRise to produce a likelihood model for genomic distance between read
171 pairs, and the model was used to identify and break putative misjoins, to score prospective joins, and
172 make joins above a threshold. After aligning and scaffolding Chicago data, Dovetail Hi-C library
173 sequences were aligned and scaffolded following the same method. After scaffolding, shotgun
174 sequences were used to close gaps between contigs.

175 The *P. monodon* genome sequence was aligned to the Pacific white shrimp *L. vannamei* (Zhang
176 et al., 2019) using Mugsy v1.2.3 (Angiuoli & Salzberg, 2011). Alignments with a length < 1 kb were
177 filtered out. The output alignments between genomes were visualized using Circos v0.69-9
178 (Krzywinski et al., 2009).

179

180 **Repetitive element analysis**

181 Species-specific repeat library was generated using RepeatModeler2 (Flynn et al., 2019) prior
182 masking with RepeatMasker (Smit, Hubley, & Green, 2013-2015). Annotation of repeats was aligned
183 to Repbase using RMBlast. All processes were performed with default parameters.

184

185 **RNA isolation, PacBio Iso-Seq library preparation sequencing and analysis**

186 Total RNA was extracted from gill, heart, hemocyte, hepatopancreas, intestine, ovary, testis,
187 pleopods, stomach and thoracic ganglia of 4-month-old shrimps using TRI REAGENT according to
188 the manufacturer's instruction (Molecular Research Center, USA). Contaminated genomic DNA was
189 removed by treatment with DNase I at 0.5 U/µg total RNA at 37 °C for 30 min. The DNA-free RNA
190 was subjected for sequencing analysis using PacBio Iso-Seq SEQUEL platform (Pacific Biosciences,
191 Menlo Park, USA, outsourced to NovogenAIT, Singapore) and ONT platform. Sequences obtained
192 from Iso-Seq were prepared as described in Pootakham study (Pootakham et al., 2020).

193

194 **Gene prediction and annotation**

195 Gene prediction and protein-coding sequence identification were performed using a
196 combination of transcriptome-based prediction, homology-based prediction and *ab initio* prediction
197 methods using EvidenceModeler (Haas et al., 2008) to generate consensus gene prediction for training
198 species-specific parameter in AUGUSTUS (Stanke, Diekhans, Baertsch, & Haussler, 2008). To locate
199 intron and exon regions, transcriptome-based prediction methods combined information from PacBio
200 Iso-seq and other available *P. monodon* transcriptome databases (PRJNA4214000, SRR1648423,
201 SRR1648424, SRR2191764, SRR2643301, SRR2643302, SRR2643304, SRR2643305) (Supporting
202 Information Table S1) to align against the genome sequence. For short-read transcripts, STAR (Dobin
203 et al., 2013) was employed to align against the genome before spliced read information was generated
204 according to a previously published protocol (Hoff & Stanke, 2019) using bam2wig script in
205 AUGUSTUS. Iso-Seq raw reads containing both 5' and 3' adapters (derived from full-length
206 transcripts) were identified, and the adapters and poly(A) sequences were trimmed. Cleaned consensus

207 reads were then mapped using Genomic Mapping and Alignment Program (GMAP) (Wu & Watanabe,
208 2005). Expressed sequence tags (Anchalee Tassanakajon et al., 2006) were aligned to the genome
209 using BLAT (Kent, 2002) and converted to potential gene structures using blat2hints script of
210 AUGUSTUS.

211 Protein sequences of *P. monodon* were mapped against proteins from closely related organisms
212 including *H. azteca*, and *L. vannamei*, using Exonerate version 2.2.0 (Slater & Birney, 2005). All gene
213 models derived from these three methods were integrated by EvidenceModeler into a high confident
214 nonredundant gene set, which was used to set species-specific parameters. Finally, AUGUSTUS was
215 used to predict genes in the genome based on the extrinsic evidence. Functional annotations of the
216 obtained gene set were conducted using Semantic Annotation Platform (SAPP) using the InterProScan
217 module (P. Jones et al., 2014; Koehorst et al., 2018) and Blast2GO (Götz et al., 2008).

218

219 **Phylogenetic analysis**

220 Mitochondria protein-coding genes were used to construct a molecular phylogenetic analysis
221 using MEGA7 software (Kumar, Stecher, & Tamura, 2016). The amino acid sequences of 22 species,
222 which were *Anopheles quadrimaculatus*, *Anopheles gambiae*, *Apis mellifera*, *Artemia franciscana*,
223 *Ceratitis capitata*, *Daphnia pulex*, *Drosophila yakuba*, *Drosophila melanogaster*, *Euthynnus affinis*,
224 *Halocaridina rubra*, *Hyalella azteca*, *Ixodes hexagonus*, *L. vannamei*, *Ligia oceanica*, *Locusta*
225 *migratoria*, *Macrobrachium rosenbergii*, *Panulirus japonicus*, *Parhyale hawaiensis*, *P. monodon*,
226 *Portunus trituberculatus*, *Rhipicephalus sanguineus*, and *Tigriopus japonicus* were used for the
227 analysis. The evolutionary history was inferred by using the maximum likelihood method based on the
228 JTT matrix-based model (D. T. Jones, Taylor, & Thornton, 1992). The tree with the highest log
229 likelihood (-84614.94) is shown. An initial tree for heuristic search was obtained automatically by
230 applying Neighbor-Join and BioNJ algorithms to a matrix of pairwise distances estimated using a JTT
231 model, and then selecting the topology with superior log likelihood value.

232 Pan-core protein families were constructed for *P. monodon* with the available crustacean
233 genome *E. affanis*, *D. pulex*, *P. hawaiensis*, *L. vannamei* and *H. azteca*. The orthologous genes protein
234 family were identified by clustering together using MMseq2 (Steinegger & Söding, 2017) with
235 standard parameters of 0.5 identity and 0.5 coverage. The pan-core protein family matrix was used to
236 construct a pan-core protein family tree follow the method presented by Snipen et al (Snipen &
237 Ussery, 2010). The comparison of common and specific protein family among the crustacean genomes
238 was present in the upset plot (Lex, Gehlenborg, Strobel, Vuillemot, & Pfister, 2014). The pan-core
239 protein family tree was used to construct an ultrametric tree using ape v5.3 library in R v3.6.1 (Paradis
240 & Schliep, 2018; R Core Team, 2019). The ultrametric tree and matrix of protein families were
241 subjected to CAFE v4.1 (Bie, Cristianini, Demuth, & Hahn, 2006) to study the evolution of gene
242 families in *P. monodon*. The resulting families were further filtered to exclude families with large
243 ranges in size (> 25) across the tree, leaving 102619 families for expansion and contraction analysis.
244 CAFE was used to obtain a maximum likelihood estimate of a global birth and death rate parameter λ
245 (lambda; the rate of gain/loss per gene per million years) across the species tree ($\lambda = 0.27$). The size of
246 families was estimated at each ancestral node and then used to obtain a family-wise p-value to indicate
247 non-random expansion or contraction for each family and across all branches of the tree.
248

249 **Transcriptome sequencing and analyses of the fast-growing and slow-growing groups**

250 The feeding trial was carried out at SGIC. Black tiger shrimps were cultured in a pond size 800
251 m^2 (25 shrimps/ m^2). Five-month-old female shrimps ($N=140$) were randomly selected for body weight
252 measurement (Supporting Information Figure S1). Two experimental groups were separated base on
253 the lowest and highest shrimp weight, called the “slow-growing” group and the “fast-growing” group,
254 respectively. Average body weight of 15 samples from the lowest body weight of the slow-growing
255 group was 13.46 ± 0.52 g, while the average body weight of 15 samples from the highest of the fast-
256 growing group was 36.27 ± 1.96 g (Supporting Information Table S2). All hepatopancreas samples
257 were immediately frozen in liquid nitrogen and stored at -80°C until use. To extract total RNA,

258 individual frozen hepatopancreas tissues were pulverized in liquid nitrogen and subjected to TRI-
259 REAGENT extraction method and DNase treatment as previously described.
260 To obtain short-read RNA sequences, 30 libraries (n=15 for each group) were constructed using
261 the HiSeq Library Preparation kit (Illumina, San Diego, USA) and sequenced using Illumina
262 NovaSeq™. Illumina sequencing using Novaseq 6000 instrument with 150 pair-end reads was
263 performed at Omics Drive, Singapore. The raw reads were quality-filtered (Q<20, >50bp) and adapter-
264 trimmed using TrimGalore (<https://github.com/FelixKrueger/TrimGalore>). The reads were mapped to
265 the genome using STAR (Dobin et al., 2013). The HTSeq-count(Anders, Pyl, & Huber, 2015) and
266 DESeq2 (Love, Huber, & Anders, 2014) provide a test for differential expression using negative
267 binomial generalized linear models, will operate to identify significant differently expressed genes
268 (DEGs) between fast- and slow-growing shrimp. DEGs were identified when their expression level
269 differences > 2.0 change with Bonferroni adjusted p-value of < 0.05. The DEGs which have read
270 count per million < 1 were discarded. Functional pathway analysis was carried using EggNOG
271 (Huerta-Cepas et al., 2019) and KEGG mapper (Kanehisa, Sato, Kawashima, Furumichi, & Tanabe,
272 2016). To determine whether the differentially expressed genes may be newly identified genes in *P.*
273 *monodon*, the sequences were aligned on available *P. monodon* protein and mRNA sequences in NCBI
274 database using BLAST (E-value $\leq 10^{-3}$). The sequences that had no match to any publicly available *P.*
275 *monodon* sequences but could be annotated were considered newly identified genes.
276 To evaluate differentially expressed genes, 15 genes (10 DEGs that had higher levels of
277 expression in the fast-growing shrimp and 5 DEGs that had higher levels of expression in the slow-
278 growing shrimp) were selected for real-time PCR analysis. Eight hepatopancreas per group (fast-
279 growing and slow-growing) were used for validation. Total RNA (1.5 μ g) was reverse transcribed into
280 cDNA using an ImPromII™ Reverse Transcriptase System kit (Promega, USA.) according to the
281 manufacturer's recommendation. Each 20 μ L qPCR reaction included 200 ng cDNA, 0.2 μ M of each
282 primer, and SsoAdvanced™ Universal SYBR® Green supermix (BioRad, USA.) according to the
283 company's instruction. The thermal cycling parameters were 95°C for 2 min 30 s, followed by 40

284 cycles of 95°C for 15 s, 58°C for 20 s and 72°C for 30 s. The melting curve analysis was performed
285 from 65°C to 95°C with a continuous fluorescent reading with a 0.5°C increment. The threshold cycle
286 (C_t) was analyzed using BioRad CFX Manager 2.1 software (BioRad, USA).

287

288 **Results**

289 **Genome sequencing, assembly and annotation**

290 A whole-genome shotgun strategy was used to sequence and assemble a black tiger shrimp
291 genome from PacBio long-read data. A total of 13,157,113 raw reads (178.94 Gb) representing 69.08X
292 coverage based on the estimated genome size of 2.59 Gb obtained from a previous report using the
293 flow cytometry method (Swathi, Shekhar, Katneni, & Vijayan, 2018). *De novo* assembly of PacBio
294 sequences yielded a preliminary assembly of 2.39 Gb (70,380 contigs) with a contig N50 of 79 kb and
295 a L50 of 6,786 contigs (Table 1). The draft genome was further assembled using the long-range
296 Chicago (*in vitro* proximity ligation; 444 million read pairs) and Hi-C (*in vivo* fixation of
297 chromosomes; 430 million read pairs) library data scaffolded with the HiRise software (Dovetail
298 Genomics, Santa Cruz, USA). The final assembly contained 44 pseudomolecules greater than 5 Mb in
299 length (hereafter referred to as chromosomes, numbered according to size; Figure 1A), corresponding
300 to the haploid chromosome number in *P. monodon* (1n = 44, 2n = 88). The 44 chromosomes covered
301 1,986,035,066 bases or 82.9% of the 2.39-Gb assembly.

302 To evaluate the quality of our *de novo* assembly, we aligned DNA short reads obtained from
303 Illumina sequencing from this work and the previous report (Yuan et al., 2018) to the assembled
304 genome and found that approximately 93% of the DNA short reads could be mapped on the here
305 reported *de novo* assembly. We also aligned the publicly available RNA-seq reads (Huerlimann et al.,
306 2018) and Iso-seq reads (Pootakham et al., 2020) to the assembly, and 90.22% and 98.77% of the
307 RNA-seq and Iso-seq reads were mapped to the assembly, respectively. To further assess the
308 completeness of the genome assembly, we checked the gene content with the BUSCO software using
309 the Eukaryota (odb9) database (Simão, Waterhouse, Ioannidis, Kriventseva, & Zdobnov, 2015). Our

310 gene prediction contained 94.72% of the highly conserved orthologs (85.15% complete, 9.57% partial,
311 5.28% missing) in the eukaryotic lineage. High mapped rates, comparable to the numbers observed in
312 *L. vannamei*, and a high percentage of identified highly conserved orthologs provided the evidence for
313 a high-quality assembly obtained for the black tiger shrimp genome.

314 The chromosome-level contiguity achieved in our assembly enabled a syntenic analysis between
315 *P. monodon* and *L. vannamei*. Portions of conserved syntenic genes between the black tiger shrimp
316 and Pacific white shrimp are illustrated in Figure 1B and 1C. The degree of macrosynteny observed
317 between these two species was consistent with the result from phylogenetic analysis showing that they
318 are very closely related and appear to have evolved from a common ancestor (Figure 1D). The
319 distribution of paralogous gene pairs revealed one-to-one synteny across 15 chromosomes/linkage
320 groups and one-to-two synteny between *P. monodon* chromosomes 4 and 30 and *L. vannamei*
321 chromosomes 14, 15, 21 and 22 (Figure 1B).

322 A combination of *ab initio* prediction, homology-based search and transcript evidence obtained
323 from both Iso-seq and RNA-seq data was used for gene prediction. The genome annotations of *P.*
324 *monodon* contained 31,640 predicted gene models, of which 30,038 were protein-coding genes (Table
325 1, Supporting Information Table S3). The number of protein-coding genes in *P. monodon* was slightly
326 higher than those reported in *L. vannamei* (25,596) (Zhang et al., 2019) and in a freshwater epibenthic
327 amphipod *Hyalella azteca* (19,936) (Poynton et al. 2018). Of 30,038 protein-coding genes, 25,569
328 (85.02%) had evidence support from our RNA-seq and Iso-seq data.

329 In addition to the nuclear genome, a complete mitochondrial genome assembly was obtained,
330 enabling phylogenetic analysis to reveal relationship with other arthropods. The assembled
331 mitochondrial genome had a size of 15,974 bp and 29.09% GC content (Supporting Information
332 Figure S2). The phylogenetic analysis of 20 arthropods based on 13 concatenated mitochondrial
333 protein-coding genes showed that *P. monodon* and other Decapoda were more closely related to the
334 insects than other crustaceans in the same class (Malacostraca) such as *H. azteca* and *Parhyale*
335 *hawaiensis* (Amphipoda), consistent with a previous study (Wilson, Cahill, Ballment, & Benzie, 2000)

336 (Figure 1D). The phylogenetic tree also showed that decapods were distantly related to crustaceans in
337 Branchiopoda class such as *Artemia franciscana* and *Daphnia pulex*.

338

339 Comparative analyses between *P. monodon* and other crustacean genomes

340 Comparative analyses of *P. monodon* genome with publicly available crustacean genomes
341 (Calanoida (*Eurytemora affinis*) (Eyun et al., 2017), Cladocera (*D. pulex*) (Colbourne et al., 2011) and
342 Amphipoda (*P. hawaiensis* (Kao et al., 2016), *L. vannamei* (Zhang et al., 2019) and *H. azteca*
343 (Poynton et al., 2018)) were performed to investigate genome evolution within the crustacean group.

344 Based on orthologous clustering by MMseq2 software (Steinegger & Söding, 2017), we identified
345 102,632 pan protein families of the crustacean with the core protein family of 583 (Figure 2A). The
346 dendrogram analysis of protein families showed a distinct group of the *Amphipoda*. As expected of the
347 closely related species, *P. monodon* and *L. vannamei* shared 5,487 common protein families that were
348 higher than those between *P. monodon* and other species. Nevertheless, both species also had around
349 11,000 species-specific protein families (Figure 2A). The numbers of expanded and contracted gene
350 numbers at each divergence event were estimated using CAFÉ software (Bie et al., 2006).

351 Considerable gene family expansions occurred on the *P. monodon* branch that might have experienced
352 additional expansions after its divergence from *H. azteca*.

353

354 Repetitive elements in *P. monodon* genome

355 The total repeat content in the black tiger shrimp genome assembly was 62.5% (Figure 2B). We
356 identified repeats comprising 572.87 Mb simple repeats (23.93%), 276.64 Mb long interspersed
357 nuclear elements (LINEs, 11.55%), 93.21 Mb long terminal repeats (LTRs, 3.89%), 75.96 Mb DNA
358 elements (3.17%), 59.09 Mb low complexity repeats (2.47%), 49.49 Mb short interspersed nuclear
359 elements (SINEs, 2.07%), 2.18 Mb small RNA (0.09%), and 368.13 Mb of unclassified repeat
360 elements (15.37%).

361 Simple repeats and LINEs are the two most abundant repeat categories in *P. monodon*, together
362 accounting for 35.48% of the genome assembly. Moreover, LINE/I (4.65%), RTE-BovB (3.59%), and
363 Penelope (0.96%) were the three major components of LINEs (Figure 2C). The major LINEs
364 components found here were in accord with the previously reported *P. monodon* genome, but with
365 different proportions (2.03%, 4.96% and 0.82% for LINE-I, RTE-BovB, and Penelope, respectively)
366 (Yuan et al., 2018).

367

368 **Identification of novel growth-associated genes**

369 Transcriptome analysis is a useful approach to identify genes that are differentially expressed
370 among individuals with various traits of interest. Without a high-quality reference genome, gene
371 expression studies have to rely on a *de novo* transcriptome assembly, which often contains a large
372 number of fragmented transcript sequences with no annotation or in some cases incorrect annotations.
373 To evaluate the utility of this high-quality genome assembly in transcriptomic analysis,
374 transcriptomics of hepatopancreas from the fast- and slow-growing shrimps were compared with and
375 without the genome assembly as a reference.

376 Comparison of the overall results from the genome assembly as a reference and from *de novo*
377 transcriptome assembly revealed a significant improvement. With the genome assembly, a lower
378 number of predicted genes with a higher N50 value was obtained (31,640 genes with N50 of 1,743 nt
379 from the genome assembly vs 340,240 genes with N50 of 776 nt from the *de novo* transcriptome
380 assembly). Moreover, a higher annotation rate (95.01%) was obtained with the genome assembly as a
381 reference than that from the *de novo* transcriptome assembly (26.36%).

382 We compared the differential gene expression profile in hepatopancreas of the fast-growing
383 shrimp and the slow-growing shrimp. This analysis identified 383 genes exhibiting higher levels of
384 expression in the fast-growing shrimp and 95 genes exhibiting higher levels in the slow-growing
385 shrimp ($\text{Log}_2 \text{ fold-change} > 1$ and $p\text{-value} < 0.05$) (Supporting Information Table S4). The fast-growing
386 shrimp grew at a faster rate and had twice the weight of the slow-growing shrimp under the same

387 rearing condition at 5 months old. To further access gene interaction networks, KEGG pathway
388 mapping was employed on the DEGs and revealed 159 pathways with an average of two genes
389 associated in each pathway (Supporting Information Table S5). The functions of DEGs were classified
390 by Clusters of Orthologous Groups (COGs) annotation into 23 categories (Supporting Information
391 Figure S3). The top five highly enriched metabolic processes were carbohydrate/lipid/amino acid
392 transport and metabolism, secondary metabolites biosynthesis, transport and catabolism, and inorganic
393 ion transport and metabolism (Figure 3A). For instance, DEGs involved in carbohydrate metabolism
394 were *amylase* (*amy*), *fructose-bisphosphate aldolase* (*aldo*), *glyceraldehyde 3-phosphate*
395 *dehydrogenase* (*gapdh*), and *insulin-like growth factor-1 receptor* (*insr*). Genes involved in lipid
396 metabolism were *nose resistant to fluoxetine* (*nrf*), *lipase* (*lip*), *glycerol-3-phosphate acyltransferase*
397 (*gpat3*), *acyl-CoA delta desaturase* (*scd*), *long-chain-fatty-acid--CoA ligase* (*acsli*) and *elongation of*
398 *very-long-chain fatty acids protein 4-like* (*elovl4*). Of all DEGs, 67 annotated genes could not be
399 matched with any *P. monodon* sequences in the publicly available genomic/transcriptomic databases
400 (Supporting Information Table S4). These newly identified genes involved in nutrient metabolic
401 processes (Figure 3A shown in blue). We further investigated pathways that have not been reported to
402 be involved in shrimp growth and found that PI3K-Akt signaling pathway has the highest number of
403 novel genes (Figure 3B). Four DEGs in PI3K-Akt signaling pathway were *integrin beta isoform 1*
404 (*itgb1*), *integrin alpha-4 like* (*itga4*), *serine/threonine-protein kinase N isoform 1* (*pkn1*) and *insr*. Of
405 these, the last three were newly identified genes.

406 To verify the transcriptome analysis, 15 DEGs with functions related to nutrient metabolism or
407 immune system were selected for quantitative real-time PCR (qPCR). The qPCR results agreed with
408 those obtained from RNA-seq with a correlation coefficient of 0.96 (Supporting Information Figure
409 S4).

410

411 **Discussion**

412 In this study, we present a whole genome sequence of *P. monodon* assembled from PacBio
413 long-read data and scaffolded using long-range Chicago and Hi-C techniques. Our chromosome-scale
414 assembly has shown tremendous improvement in contiguity and completeness compared to the
415 previously reported *P. monodon* genomes (Quyen et al., 2020; Yuan et al., 2018). Based on a
416 benchmark (10Mb) (Reference standard for genome biology, 2018), the assembly presented here is
417 considered a high-quality reference genome as it has the N50 scaffold length of 44.86 Mb. It is also
418 one of the highest quality crustacean genomes currently available. Of the 45 crustacean genome
419 sequences listed in the NCBI genome database, only three species (*Tigriopus japonicus*, *T.*
420 *californicus* and *Daphnia magna*) have their genomes assembled at a chromosome level.

421 The present genome provides an invaluable resource for shrimp research. The availability of the
422 chromosome-scale assembly allowed us to examine the synteny relationship between the two
423 economically important penaeid shrimp species: the black tiger shrimp and the Pacific white shrimp
424 genomes. The synteny analysis revealed a one-to-one relationship between *P. monodon* and *L.*
425 *vannamei* chromosomes, suggesting that certain chromosomes derived from the common ancestor of
426 *P. monodon* and *L. vannamei* were fragmented into two smaller chromosomes in *L. vannamei* (for
427 example, *P. monodon* chromosome 4 displayed synteny to *L. vannamei* pseudochromosomes 14 and
428 15; Figure 1B) but remained as single chromosomes in *P. monodon*.

429 Obtaining contiguous long-read-based genome of shrimp has been hampered by limitation
430 related to short-read sequencing technology. PacBio sequencing reads allow the assembler to obtain a
431 contiguous assembly that spans repeat regions containing transposable elements and tandem repeats.
432 We found that *P. monodon* has the highest repeat abundance (62.5%) when compared to five available
433 genome sequences of crustacean species: *L. vannamei* (53.9%), *P. hawaiensis* (44.7%), *E. affinis*
434 (40.2%), *H. azteca* (24.3%) and *D. pulex* (22.0%). Moreover, the percentage of repeat elements
435 observed in this assembly was substantially higher than reported in previous studies on *P. monodon*
436 fosmid (51.8%) (Huang et al., 2011) and genome (46.8%) (Yuan et al., 2018). High repeat contents
437 and long repetitive sequences hinder genome assembly. Ambiguous regions containing mostly

438 repetitive sequences might be missed or caused errors in assembly using short sequencing reads
439 employed in the previous assembly of the *P. monodon* genomes (Yuan et al., 2018) and *L. vannamei*
440 genome (Zhang et al., 2019). Our assembly, on the other hand, utilized the PacBio sequencing
441 platform, which yielded kilobase-sized reads that could be assembled into contigs and scaffolds large
442 enough to span repetitive regions, alleviating the problems often encountered by the use of short-read
443 technologies.

444 The chromosome-scale assembly allows for an in-depth investigation of repeat elements. Even
445 though the biological function of repeats has not been well studied in the shrimp, they might be
446 associated with important functions as reported in other organisms. For example, LINE/I plays a role
447 on transcription in human by co-mobilizing DNA to new locations (Pickeral, Makałowski, Boguski, &
448 Boeke, 2000). Among diverse repetitive elements, LINE was the major element in both *P. monodon*
449 and *L. vannamei*. The most abundant element in *P. monodon* and *L. vannamei* were LINE/I and
450 LINE/L2, respectively. Given that the diversity of repeats was deemed to play a role in environmental
451 adaptation of animals (Schrader & Schmitz, 2019), roles of these repetitive elements in the black tiger
452 shrimp could be further explored to gain a better understanding of shrimp biology.

453 Another advantage of the high-quality reference genome is the reduction in erroneous and
454 fragmented assembled contigs using *de novo* transcripts. With this high-quality reference genome
455 assembly, we were able to obtain an improved gene set with better contiguity and annotation rate. Of
456 the predicted genes in the genome, 95.01% of them could be functionally annotated. The results
457 suggested that our genome assembly could serve as a high-quality reference for facilitating functional
458 genomic study in the black tiger shrimp.

459 The chromosome-scale assembly facilitates downstream applications for molecular breeding
460 and gene expression studies in shrimp. Growth is undoubtedly an important factor for profitable
461 shrimp production. However, a daunting challenge in black tiger shrimp farming is its slower growth
462 rate in captivity (Benzie, Kenway, & Ballment, 2001; Cheng & Chen, 1990). Domesticated shrimps
463 could not mature well with declining growth rates over generations (Jackson & Wang, 1998). Albeit

464 its importance, the knowledge on genes controlling shrimp's growth remained limited partly due to the
465 lack of the genome, thus up-to-now most growth-related genes identified in *P. monodon* were from *L.*
466 *vannamei* (Gao et al., 2017; Gao et al., 2015; Santos et al., 2018).

467 The comparison of hepatopancreas transcriptomes of slow-growing shrimp and fast-growing
468 shrimp revealed that DEGs were mainly involved in nutrient metabolism, which was in concordance
469 with the hepatopancreas functions in feed utilization and energy storage. Here, we presented genes
470 related to carbohydrate and lipid metabolisms as they are main nutrients that have been investigated to
471 enhance growth in shrimp (Coelho, Yasumaru, Passos, Gomes, & Lemos, 2019; González-Félix,
472 Gatlin, Lawrence, & Perez-Velazquez, 2002; Hu et al., 2019; Olmos, Ochoa, Paniagua-Michel, &
473 Contreras, 2011). Genes with higher expression levels in the fast-growing group were found to be
474 involved in nutrient metabolism and secondary metabolite biosynthesis. Genes exhibiting higher levels
475 of expression in the fast-growing shrimp were digestive enzymes such as amylase and lipase, in
476 agreement with the prior finding that enhancement of digestive enzyme activities improves growth
477 performance of shrimp activities (Anand et al., 2013; Gómez & Shen, 2008). As dietary carbohydrates
478 can enhance growth (Sagar et al., 2019), it is not surprising to find carbohydrate metabolism genes
479 such as *aldo*, *gapdh* and *insr* expressed at a higher level in the fast-growing shrimp

480 Similarly, DEGs in lipid metabolism agree with the established knowledge on the importance of
481 fatty acids and lipids to the shrimp growth and immunity (Chen et al., 2015; Duan et al., 2019; Toledo,
482 Silva, Vieira, Mourão, & Seiffert, 2016). Many fatty acids such as highly unsaturated fatty acids
483 (HUFA) are indeed essential to marine animals since they are the major component of cell membrane
484 (An et al., 2020). Thus, regulation of the synthesis, digestion and absorption of these fatty acids is a
485 key to shrimp growth. The higher expression of genes involved in unsaturated fatty acid (UFA)
486 biosynthesis such as *scd* and *acs1l* in the fast-growing group suggested that these fatty acids might
487 positively associate with growth. The results agree with the previous studies reported that additional of
488 high HUFA such as linoleic (LOA, 18:2n-6), linolenic (LNA, 18:3n-3), eicosapentaenoic acid (EPA,
489 20:5n-3) or docosahexaenoic acid (DHA, 22:6n-3) in diet could promote the growth (Glencross,

490 Smith, Thomas, & Williams, 2002a, 2002b). Interestingly, *elovl4* that synthesizes very long-chain
491 (>C24) saturated and polyunsaturated fatty acids (Oboh, Navarro, Tocher, & Monroig, 2017) was
492 expressed at a higher level in the slow-growing shrimp than in the fast-growing one. In gilthead sea
493 bream *Sparus aurata*, high amount of LNA and long-chain fatty acid adversely affected growth
494 (Turkmen et al., 2019). Considering the above data, it could be implied that balance lipid composition
495 is an important factor controlling growth performance; thus, feed formulation to promote growth
496 should be optimized by considering lipid ratios.

497 Among the DEGs, three new candidate marker genes may potentially be useful for shrimp
498 breeding programs, namely *tranferin (trf)*, *nrf* and *pkn1*. Trf is an insulin-like growth factor (IGF) that
499 stimulates both proliferation and differentiation in a cell line (Kiepe, Ciarmatori, Hoeflich, Wolf, &
500 Tonshoff, 2005), making it a promising candidate as a growth marker. Nrf, a lipid-carrier protein,
501 has been reported to be essential for embryonic development in *Caenorhabditis elegans* (Watts &
502 Browse, 2006). Given the aforementioned importance of lipid for shrimp growth, Nrf might regulate
503 the intake and storage of lipid for the growth. Besides nutrient metabolic pathways, PI3K-Akt pathway
504 presents an interesting pathway for further investigation for its involvement in growth regulation as we
505 found three novel genes (*pkn1*, *itga4*, and *insr*) in this pathway. PI3K-Akt is a regulatory pathway
506 controlling glucose balance by cross-talking with insulin signaling pathway (Shi & He, 2016).
507 Although an association between PI3K-Akt and shrimp growth performance has not yet been
508 investigated in *P. monodon*, there has been a report that PI3K-Akt is linked to growth factors and
509 cellular survival (Choi et al., 2019; Dai, Li, Fu, Qiu, & Chen, 2020; Fuentes, Valdés, Molina, &
510 Björnsson, 2013). Here, novel genes associated with PI3K-Akt pathway showed higher expression in
511 the fast-growing shrimp; therefore, it suggested that these genes might have potential roles in
512 promoting growth. Particularly, the distinct expression values of *pkn1* between fast- and slow-growing
513 shrimps make it interesting for further study (Supporting Information Figure S4). Pkn1 is found in
514 various tissues with different functions in many animals (Mukai, 2003). For instance, Pkn1 in testis
515 regulates male fertility of the Pacific abalone *Haliotis discus hannai*, (Kim, Kim, Park, & Nam, 2019),

516 whereas it has been linked to the regulation of actin and cytoskeletal network in human (Dong et al.,
517 2000). These newly identified candidate genes might provide better understanding of shrimp growth
518 and facilitate black tiger shrimp genomic breeding programs.

519 In conclusion, we have successfully overcome the technical challenges in obtaining the first
520 high-quality chromosome-scale genome assembly of the economically important *P. monodon*. The
521 availability of this reference genome enables several downstream biological and industrial applications
522 that would otherwise be difficult. This reference genome will benefit not only the *P. monodon* research
523 community, but also other researchers working on related shrimp and crustacean species. Moreover,
524 the newly identified growth-associated genes might help advance the understanding of growth in the
525 black tiger shrimp and facilitate its genomic breeding programs.

526

527 **Acknowledgements**

528 The authors acknowledge NSTDA Supercomputer Center (ThaiSC) for providing HPC
529 resources that have contributed to the research results reported within this paper. We thank Ms. Somjai
530 Wongtripop, Mr. Kaitisak kaewlok and Shrimp Genetic Improvement Center (SGIC) members, as
531 well as Ms. Sudtida Phuengwas (BIOTEC) for the shrimp sample collection. This project was funded
532 by National Center for Genetic Engineering and Biotechnology (BIOTEC Platform No. P1651718),
533 TDG Food and Feed program, National Science and Technology Development Agency (No.
534 P1950419) and partially supported by the European Union's Horizon 2020 research and innovation
535 programme under the Marie Skłodowska-Curie grant agreement No 734486 (SAFE-Aqua). Visiting
536 Professor Program 2019 was awarded to Dr. Intawat Nookaew by the National Science and
537 Technology Development Agency, Thailand. We acknowledge Zulema Dominguez (University of
538 Arkansas for Medical Sciences, USA) for technical assistance on comparative genome. We are
539 grateful to Prof. Morakot Tanticharoen (NSTDA), Dr. Kanyawim Kirtikara (BIOTEC), Dr. Wonnop
540 Visessanguan (BIOTEC) and Assoc Prof. Skorn Koonawootrittriron (Kasetsart University, Thailand)
541 for their mentorship on the shrimp research programs.

542

543 **References**

- 544
- 545 An, W., He, H., Dong, X., Tan, B., Yang, Q., Chi, S., . . . Yang, Y. (2020). Regulation of growth, fatty
546 acid profiles, hematological characteristics and hepatopancreatic histology by different dietary
547 n-3 highly unsaturated fatty acids levels in the first stages of juvenile Pacific white shrimp
548 (*Litopenaeus vannamei*). *Aquaculture Reports*, 17, 100321. doi:10.1016/j.aqrep.2020.100321
- 549 Anand, P. S. S., Kohli, M. P. S., Roy, S. D., Sundaray, J. K., Kumar, S., Sinha, A., . . . Sukham, M. k.
550 (2013). Effect of dietary supplementation of periphyton on growth performance and digestive
551 enzyme activities in *Penaeus monodon*. *Aquaculture*, 392-395, 59-68.
552 doi:10.1016/j.aquaculture.2013.01.029
- 553 Anders, S., Pyl, P. T., & Huber, W. (2015). HTSeq--a Python framework to work with high-
554 throughput sequencing data. *Bioinformatics*, 31(2), 166-169.
555 doi:10.1093/bioinformatics/btu638
- 556 Anderson, J. L. (2019, 4 November 2019). GOAL 2019: Global shrimp production review. Retrieved
557 from <https://www.aquaculturealliance.org/advocate/goal-2019-global-shrimp-production-review/>
- 558
- 559 Angiuoli, S. V., & Salzberg, S. L. (2011). Mugsy: fast multiple alignment of closely related whole
560 genomes. *Bioinformatics*, 27(3), 334-342. doi:10.1093/bioinformatics/btq665
- 561 Baranski, M., Gopikrishna, G., Robinson, N. A., Katneni, V. K., Shekhar, M. S., Shanmugakarthik, J.,
562 . . . Ponniah, A. G. (2014). The development of a high density linkage map for black tiger
563 shrimp (*Penaeus monodon*) based on cSNPs. *PLoS One*, 9(1), e85413.
564 doi:10.1371/journal.pone.0085413
- 565 Benzie, J. A. H., Kenway, M., & Ballment, E. (2001). Growth of *Penaeus monodon* x *Penaeus*
566 *esculentus* tiger prawn hybrids relative to the parental species. *Aquaculture*, 193(3-4), 227-
567 237. doi:10.1016/s0044-8486(00)00487-7
- 568 Bie, T. D., Cristianini, N., Demuth, J. P., & Hahn, M. W. (2006). CAFE: a computational tool for the
569 study of gene family evolution. *Bioinformatics*, 22(10), 1269-1271.
570 doi:10.1093/bioinformatics/btl097
- 571 Brooker, A. L., Benzie, J. A. H., Blair, D., & Versini, J. J. (2000). Population structure of the giant
572 tiger prawn *Penaeus monodon* in Australian waters, determined using microsatellite markers.
573 *Marine Biology*, 136(1), 149-157. doi:10.1007/s002270050017
- 574 Chen, K., Li, E., Xu, C., Wang, X., Lin, H., Qin, J. G., & Chen, L. (2015). Evaluation of different lipid
575 sources in diet of pacific white shrimp *Litopenaeus vannamei* at low salinity. *Aquaculture*
576 *Reports*, 2, 163-168. doi:10.1016/j.aqrep.2015.10.003
- 577 Cheng, C. S., & Chen, L.-c. (1990). Growth characteristics and relationships among body length, body
578 weight and tail weight of *Penaeus monodon* from a culture environment in Taiwan.
579 *Aquaculture*, 91(3-4), 253-263. doi:10.1016/0044-8486(90)90192-p
- 580 Choi, E., Kikuchi, S., Gao, H., Brodzik, K., Nassour, I., Yopp, A., . . . Yu, H. (2019). Mitotic
581 regulators and the SHP2-MAPK pathway promote IR endocytosis and feedback regulation of
582 insulin signaling. *Nat Commun*, 10(1), 1473. doi:10.1038/s41467-019-09318-3
- 583 Coelho, R. T. I., Yasumaru, F. A., Passos, M. J. A. C. R., Gomes, V., & Lemos, D. (2019). Energy
584 budgets for juvenile Pacific whiteleg shrimp *Litopenaeus vannamei* fed different diets.
585 *Brazilian Journal of Oceanography*, 67, e19243. doi:10.1590/s1679-87592019024306701
- 586 Colbourne, J. K., Pfrender, M. E., Gilbert, D., Thomas, W. K., Tucker, A., Oakley, T. H., . . . Boore, J.
587 L. (2011). The ecoresponsive genome of *Daphnia pulex*. *Science*, 331(6017), 555-561.
588 doi:10.1126/science.1197761
- 589 Dai, M., Li, S., Fu, C., Qiu, H., & Chen, N. (2020). The potential role of marine protein hydrolyzates
590 in elevating nutritive values of diets for largemouth bass, *Micropterus salmoides*. *Frontiers in*
591 *Marine Science*, 7, 197 doi:10.3389/fmars.2020.00197

- 592 Dobin, A., Davis, C. A., Schlesinger, F., Drenkow, J., Zaleski, C., Jha, S., . . . Gingeras, T. R. (2013).
593 STAR: ultrafast universal RNA-seq aligner. *Bioinformatics*, 29(1), 15-21.
594 doi:10.1093/bioinformatics/bts635
- 595 Dong, L. Q., Landa, L. R., Wick, M. J., Zhu, L., Mukai, H., Ono, Y., & Liu, F. (2000).
596 Phosphorylation of protein kinase N by phosphoinositide-dependent protein kinase-1 mediates
597 insulin signals to the actin cytoskeleton. *Proceedings of the National Academy of Sciences of
598 the United States of America*, 97(10), 5089-5094. doi:10.1073/pnas.090491897
- 599 Duan, Y., Wang, Y., Liu, Q., Dong, H., Li, H., Xiong, D., & Zhang, J. (2019). Changes in the intestine
600 microbial, digestion and immunity of *Litopenaeus vannamei* in response to dietary resistant
601 starch. *Scientific Reports*, 9(1), 6464. doi:10.1038/s41598-019-42939-8
- 602 Eyun, S.-I., Soh, H. Y., Posavi, M., Munro, J. B., Hughes, D. S. T., Murali, S. C., . . . Lee, C. E.
603 (2017). Evolutionary history of chemosensory-related gene families across the Arthropoda.
604 *Molecular Biology and Evolution*, 34(8), 1838-1862. doi:10.1093/molbev/msx147
- 605 FAO. (2018). The State of World Fisheries and Aquaculture 2018 - Meeting the sustainable
606 development goals [Press release]
- 607 Flynn, J. M., Hubley, R., Goubert, C., Rosen, J., Clark, A. G., Feschotte, C., & Smit, A. F. (2019).
608 RepeatModeler2: automated genomic discovery of transposable element families. *bioRxiv*,
609 856591. doi:10.1101/856591
- 610 Fuentes, E. N., Valdés, J. A., Molina, A., & Björnsson, B. T. (2013). Regulation of skeletal muscle
611 growth in fish by the growth hormone – Insulin-like growth factor system. *General and
612 Comparative Endocrinology*, 192, 136-148. doi:10.1016/j.ygcen.2013.06.009
- 613 Gao, Y., Wei, J., Yuan, J., Zhang, X., Li, F., & Xiang, J. (2017). Transcriptome analysis on the
614 exoskeleton formation in early developmental stages and reconstruction scenario in growth-
615 moulting in *Litopenaeus vannamei*. *Scientific Reports*, 7(1), 1098. doi:10.1038/s41598-017-
616 01220-6
- 617 Gao, Y., Zhang, X., Wei, J., Sun, X., Yuan, J., Li, F., & Xiang, J. (2015). Whole transcriptome
618 analysis provides insights into molecular mechanisms for molting in *Litopenaeus vannamei*.
619 *PLoS One*, 10(12), e0144350. doi:10.1371/journal.pone.0144350
- 620 Glencross, B. D., Smith, D. M., Thomas, M. R., & Williams, K. C. (2002a). The effect of dietary n-3
621 and n-6 fatty acid balance on the growth of the prawn *Penaeus monodon*. *Aquaculture
622 Nutrition*, 8(1), 43-51. doi:10.1046/j.1365-2095.2002.00188.x
- 623 Glencross, B. D., Smith, D. M., Thomas, M. R., & Williams, K. C. (2002b). Optimising the essential
624 fatty acids in the diet for weight gain of the prawn, *Penaeus monodon*. *Aquaculture*, 204(1-2),
625 85-99. doi:10.1016/s0044-8486(01)00644-5
- 626 Gómez, R. G. D., & Shen, M. A. (2008). Influence of probiotics on the growth and digestive enzyme
627 activity of white Pacific shrimp (*Litopenaeus vannamei*). *Journal of Ocean University of
628 China*, 7(2), 215-218. doi:10.1007/s11802-008-0215-x
- 629 González-Félix, M. L., Gatlin, D. M., Lawrence, A. L., & Perez-Velazquez, M. (2002). Effect of
630 dietary phospholipid on essential fatty acid requirements and tissue lipid composition of
631 *Litopenaeus vannamei* juveniles. *Aquaculture*, 207(1-2), 151-167. doi:10.1016/s0044-
632 8486(01)00797-9
- 633 Götz, S., García-Gómez, J. M., Terol, J., Williams, T. D., Nagaraj, S. H., Nueda, M. J., . . . Conesa, A.
634 (2008). High-throughput functional annotation and data mining with the Blast2GO suite.
635 *Nucleic Acids Research*, 36(10), 3420-3435. doi:10.1093/nar/gkn176
- 636 Guppy, J. L., Jones, D. B., Jerry, D. R., Wade, N. M., Raadsma, H. W., Huerlimann, R., & Zenger, K.
637 R. (2018). The state of “Omics” research for farmed penaeids: advances in research and
638 impediments to industry utilization. *Frontiers in Genetics*, 9, 282.
639 doi:10.3389/fgene.2018.00282
- 640 Haas, B. J., Salzberg, S. L., Zhu, W., Pertea, M., Allen, J. E., Orvis, J., . . . Wortman, J. R. (2008).
641 Automated eukaryotic gene structure annotation using EVidenceModeler and the program to
642 assemble spliced alignments. *Genome Biology*, 9(1), R7. doi:10.1186/gb-2008-9-1-r7

- 643 Hoff, K. J., & Stanke, M. (2019). Predicting genes in single genomes with AUGUSTUS. *Current*
644 *Protocols in Bioinformatics*, 65(1), e57. doi:10.1002/cpb.57
- 645 Hu, X., Yang, H.-L., Yan, Y.-Y., Zhang, C.-X., Ye, J.-d., Lu, K.-L., . . . Sun, Y.-Z. (2019). Effects of
646 fructooligosaccharide on growth, immunity and intestinal microbiota of shrimp (*Litopenaeus*
647 *vannamei*) fed diets with fish meal partially replaced by soybean meal. *Aquaculture Nutrition*,
648 25(1), 194-204. doi:10.1111/anu.12843
- 649 Huang, S.-W., Lin, Y.-Y., You, E.-M., Liu, T.-T., Shu, H.-Y., Wu, K.-M., . . . Yu, H.-T. (2011).
650 Fosmid library end sequencing reveals a rarely known genome structure of marine shrimp
651 *Penaeus monodon*. *BMC Genomics*, 12(1), 242. doi:10.1186/1471-2164-12-242
- 652 Huerlimann, R., Wade, N. M., Gordon, L., Montenegro, J. D., Goodall, J., McWilliam, S., . . . Jerry,
653 D. R. (2018). De novo assembly, characterization, functional annotation and expression
654 patterns of the black tiger shrimp (*Penaeus monodon*) transcriptome. *Scientific Reports*, 8(1),
655 13553. doi:10.1038/s41598-018-31148-4
- 656 Huerta-Cepas, J., Szklarczyk, D., Heller, D., Hernández-Plaza, A., Forslund, S. K., Cook, H., . . .
657 Bork, P. (2019). eggNOG 5.0: a hierarchical, functionally and phylogenetically annotated
658 orthology resource based on 5090 organisms and 2502 viruses. *Nucleic Acids Research*,
659 47(D1), D309-D314. doi:10.1093/nar/gky1085
- 660 Jackson, C. J., & Wang, Y. G. (1998). Modelling growth rate of *Penaeus monodon Fabricius* in
661 intensively managed ponds: effects of temperature, pond age and stocking density.
662 *Aquaculture Research*, 29(1), 27-36. doi:10.1111/j.1365-2109.1998.tb01358.x
- 663 Jones, D. T., Taylor, W. R., & Thornton, J. M. (1992). The rapid generation of mutation data matrices
664 from protein sequences. *Bioinformatics*, 8(3), 275-282. doi:10.1093/bioinformatics/8.3.275
- 665 Jones, P., Binns, D., Chang, H.-Y., Fraser, M., Li, W., McAnulla, C., . . . Hunter, S. (2014).
666 InterProScan 5: genome-scale protein function classification. *Bioinformatics*, 30(9), 1236-
667 1240. doi:10.1093/bioinformatics/btu031
- 668 Kanehisa, M., Sato, Y., Kawashima, M., Furumichi, M., & Tanabe, M. (2016). KEGG as a reference
669 resource for gene and protein annotation. *Nucleic Acids Research*, 44(D1), D457-462.
670 doi:10.1093/nar/gkv1070
- 671 Kao, D., Lai, A. G., Stamatakis, E., Rosic, S., Konstantinides, N., Jarvis, E., . . . Aboobaker, A. (2016).
672 The genome of the crustacean *Parhyale hawaiensis*, a model for animal development,
673 regeneration, immunity and lignocellulose digestion. *eLife*, 5, e20062.
674 doi:10.7554/eLife.20062
- 675 Karoonuthaisiri, N., Sittikankeaw, K., Preechaphol, R., Kalachikov, S., Wongsurawat, T.,
676 Uawisetwathana, U., . . . Kirtikara, K. (2009). ReproArray(GTS): a cDNA microarray for
677 identification of reproduction-related genes in the giant tiger shrimp *Penaeus monodon* and
678 characterization of a novel nuclear autoantigenic sperm protein (NASP) gene. *Comparative
679 Biochemistry and Physiology - Part D: Genomics and Proteomics*, 4(2), 90-99.
680 doi:10.1016/j.cbd.2008.11.003
- 681 Kent, W. J. (2002). BLAT--the BLAST-like alignment tool. *Genome Res*, 12(4), 656-664.
682 doi:10.1101/gr.229202
- 683 Kiepe, D., Ciarmatori, S., Hoeflich, A., Wolf, E., & Tonshoff, B. (2005). Insulin-like growth factor
684 (IGF)-I stimulates cell proliferation and induces IGF binding protein (IGFBP)-3 and IGFBP-5
685 gene expression in cultured growth plate chondrocytes via distinct signaling pathways.
686 *Endocrinology*, 146(7), 3096-3104. doi:10.1210/en.2005-0324
- 687 Kim, E. J., Kim, S. J., Park, C. J., & Nam, Y. K. (2019). Characterization of testis-specific
688 serine/threonine kinase 1-like (TSSK1-like) gene and expression patterns in diploid and
689 triploid Pacific abalone (*Haliotis discus hawaii*; Gastropoda; Mollusca) males. *PLoS One*,
690 14(12), e0226022. doi:10.1371/journal.pone.0226022
- 691 Koehorst, J. J., van Dam, J. C. J., Saccenti, E., Martins Dos Santos, V. A. P., Suarez-Diez, M., &
692 Schaap, P. J. (2018). SAPP: functional genome annotation and analysis through a semantic
693 framework using FAIR principles. *Bioinformatics*, 34(8), 1401-1403.
694 doi:10.1093/bioinformatics/btx767

- 695 Krzywinski, M., Schein, J., Birol, I., Connors, J., Gascoyne, R., Horsman, D., . . . Marra, M. A.
696 (2009). Circos: an information aesthetic for comparative genomics. *Genome Res*, 19(9), 1639-
697 1645. doi:10.1101/gr.092759.109
- 698 Kumar, S., Stecher, G., & Tamura, K. (2016). MEGA7: Molecular Evolutionary Genetics Analysis
699 Version 7.0 for Bigger Datasets. *Molecular Biology and Evolution*, 33(7), 1870-1874.
700 doi:10.1093/molbev/msw054
- 701 Leelatanawit, R., Uawisetwathana, U., Klinbunga, S., & Karoonuthaisiri, N. (2011). A cDNA
702 microarray, UniShrimpChip, for identification of genes relevant to testicular development in
703 the black tiger shrimp (*Penaeus monodon*). *BMC Molecular Biology*, 12, 15.
704 doi:10.1186/1471-2199-12-15
- 705 Lehnert, S. A., Wilson, K. J., Byrne, K., & Moore, S. S. (1999). Tissue-Specific Expressed Sequence
706 Tags from the Black Tiger Shrimp *Penaeus monodon*. *Mar Biotechnol*, 1(5), 465-0476.
- 707 Lex, A., Gehlenborg, N., Strobelt, H., Vuillemot, R., & Pfister, H. (2014). UpSet: Visualization of
708 Intersecting Sets. *IEEE Transactions on Visualization and Computer Graphic*, 20(12), 1983-
709 1992. doi:10.1109/TVCG.2014.2346248
- 710 Li, H. (2018). Minimap2: pairwise alignment for nucleotide sequences. *Bioinformatics*, 34(18), 3094-
711 3100. doi:10.1093/bioinformatics/bty191
- 712 Lieberman-Aiden, E., van Berkum, N. L., Williams, L., Imakaev, M., Ragoczy, T., Telling, A., . . .
713 Dekker, J. (2009). Comprehensive mapping of long-range interactions reveals folding
714 principles of the human genome. *Science*, 326(5950), 289-293. doi:10.1126/science.1181369
- 715 Love, M. I., Huber, W., & Anders, S. (2014). Moderated estimation of fold change and dispersion for
716 RNA-seq data with DESeq2. *Genome Biology*, 15(12), 550. doi:10.1186/s13059-014-0550-8
- 717 Mukai, H. (2003). The structure and function of PKN, a protein kinase having a catalytic domain
718 homologous to that of PKC. *The Journal of Biochemistry*, 133(1), 17-27.
719 doi:10.1093/jb/mvg019
- 720 Oboh, A., Navarro, J. C., Tocher, D. R., & Monroig, O. (2017). Elongation of very long-chain (>C24)
721 fatty acids in clarias gariepinus: cloning, functional characterization and tissue expression of
722 elovl4 elongases. *Lipids*, 52(10), 837-848. doi:10.1007/s11745-017-4289-3
- 723 Olmos, J., Ochoa, L., Paniagua-Michel, J., & Contreras, R. (2011). Functional feed assessment on
724 *Litopenaeus vannamei* using 100% fish meal replacement by soybean meal, high levels of
725 complex carbohydrates and *Bacillus* probiotic strains. *Marine Drugs*, 9(6), 1119-1132.
726 doi:10.3390/md9061119
- 727 Paradis, E., & Schliep, K. (2018). ape 5.0: an environment for modern phylogenetics and evolutionary
728 analyses in R. *Bioinformatics*, 35(3), 526-528. doi:10.1093/bioinformatics/bty633
- 729 Pickeral, O. K., Makałowski, W., Boguski, M. S., & Boeke, J. D. (2000). Frequent human genomic
730 DNA transduction driven by LINE-1 retrotransposition. *Genome Res*, 10(4), 411-415.
731 doi:10.1101/gr.10.4.411
- 732 Pootakham, W., Uengwetwanit, T., Sonthirod, C., Sittikankaew, K., & Karoonuthaisiri, N. (2020). A
733 novel full-Length transcriptome resource for black tiger shrimp (*Penaeus monodon*)
734 developed using isoform sequencing (Iso-Seq). *Frontiers in Marine Science*, 7, 172.
735 doi:10.3389/fmars.2020.00172
- 736 Poynton, H. C., Hasenbein, S., Benoit, J. B., Sepulveda, M. S., Poelchau, M. F., Hughes, D. S. T., . . .
737 Richards, S. (2018). The toxicogenome of *Hyalella azteca*: a model for sediment
738 ecotoxicology and evolutionary toxicology. *Environmental Science & Technology*, 52(10),
739 6009-6022. doi:10.1021/acs.est.8b00837
- 740 Putnam, N. H., O'Connell, B. L., Stites, J. C., Rice, B. J., Blanchette, M., Calef, R., . . . Green, R. E.
741 (2016). Chromosome-scale shotgun assembly using an in vitro method for long-range linkage.
742 *Genome Res*, 26(3), 342-350. doi:10.1101/gr.193474.115
- 743 Quyen, D. V., Gan, H. M., Lee, Y. P., Nguyen, D. D., Nguyen, T. H., Tran, X. T., . . . Austin, C. M.
744 (2020). Improved genomic resources for the black tiger prawn (*Penaeus monodon*). *Marine
745 Genomics*, 100751.

- 746 R Core Team. (2019). R: a language and environment for statistical computing. Vienna, Austria: R
747 Foundation for Statistical Computing. Retrieved from <https://www.R-project.org/>
- 748 Reference standard for genome biology. (2018). A reference standard for genome biology. *Nature*
749 *Biotechnology*, 36(12), 1121-1121. doi:10.1038/nbt.4318
- 750 Sagar, V., Sahu, N. P., Pal, A. K., Hassaan, M., Jain, K. K., Salim, H. S., . . . El-Haroun, E. R. (2019).
751 Effect of different stock types and dietary protein levels on key enzyme activities of
752 glycolysis-gluconeogenesis, the pentose phosphate pathway and amino acid metabolism in
753 *Macrobrachium rosenbergii*. *Journal of Applied Ichthyology*, 35(4), 1016-1024.
754 doi:10.1111/jai.13931
- 755 Santos, C. A., Andrade, S. C. S., Teixeira, A. K., Farias, F., Kurkjian, K., Guerrelhas, A. C., . . .
756 Freitas, P. D. (2018). *Litopenaeus vannamei* transcriptome profile of populations evaluated for
757 growth performance and exposed to white spot syndrome virus (WSSV). *Frontiers in*
758 *Genetics*, 9(120). doi:10.3389/fgene.2018.00120
- 759 Schrader, L., & Schmitz, J. (2019). The impact of transposable elements in adaptive evolution.
760 *Molecular Ecology*, 28(6), 1537-1549. doi:10.1111/mec.14794
- 761 Shi, Y., & He, M.-x. (2016). PfIRR Interacts with HrIGF-I and activates the MAP-kinase and PI3-
762 kinase signaling pathways to regulate glycogen metabolism in *Pinctada fucata*. *Scientific*
763 *Reports*, 6(1), 22063. doi:10.1038/srep22063
- 764 Simão, F. A., Waterhouse, R. M., Ioannidis, P., Kriventseva, E. V., & Zdobnov, E. M. (2015).
765 BUSCO: assessing genome assembly and annotation completeness with single-copy
766 orthologs. *Bioinformatics*, 31, 3210-3212.
- 767 Sittikankaew, K., Pootakham, W., Sonthirod, C., Sangsakru, D., Yoocha, T., Khudet, J., . . .
768 Karoonuthaisiri, N. (2020). Transcriptome analyses reveal the synergistic effects of feeding
769 and eyestalk ablation on ovarian maturation in black tiger shrimp. *Scientific Reports*, 10(1),
770 3239. doi:10.1038/s41598-020-60192-2
- 771 Slater, G. S. C., & Birney, E. (2005). Automated generation of heuristics for biological sequence
772 comparison. *BMC Bioinform*, 6(1), 31. doi:10.1186/1471-2105-6-31
- 773 Smit, A., Hubley, R., & Green, P. (2013-2015). RepeatMasker Open-4.0.
774 <http://www.repeatmasker.org>.
- 775 Snipen, L., & Ussery, D. W. (2010). Standard operating procedure for computing pangenome trees.
776 *Standards in Genomic Sciences*, 2(1), 135-141. doi:10.4056/sigs.38923
- 777 Stanke, M., Diekhans, M., Baertsch, R., & Haussler, D. (2008). Using native and syntenically mapped
778 cDNA alignments to improve de novo gene finding. *Bioinformatics*, 24(5), 637-644.
779 doi:10.1093/bioinformatics/btn013
- 780 Steinegger, M., & Söding, J. (2017). MMseqs2 enables sensitive protein sequence searching for the
781 analysis of massive data sets. *Nature Biotechnology*, 35(11), 1026-1028. doi:10.1038/nbt.3988
- 782 Supungul, P., Klinbunga, S., Pichyangkura, R., Jitrapakdee, S., Hirono, I., Aoki, T., & Tassanakajon,
783 A. (2002). Identification of immune-related genes in hemocytes of black tiger shrimp
784 (*Penaeus monodon*). *Mar Biotechnol*, 4(5), 487-494. doi:10.1007/s10126-002-0043-8
- 785 Swathi, A., Shekhar, M. S., Katneni, V. K., & Vijayan, K. K. (2018). Genome size estimation of
786 brackishwater fishes and penaeid shrimps by flow cytometry. *Molecular Biology Reports*,
787 45(5), 951-960. doi:10.1007/s11033-018-4243-3
- 788 Tassanakajon, A., Klinbunga, S., Paunglarp, N., Rimphanitchayakit, V., Udomkit, A., Jitrapakdee, S., .
789 . . Lursinsap, C. (2006). *Penaeus monodon* gene discovery project: The generation of an EST
790 collection and establishment of a database. *Gene*, 384, 104-112.
791 doi:10.1016/j.gene.2006.07.012
- 792 Tassanakajon, A., Pongsomboon, S., Jarayabhand, P., Klinbunga, S., & Boonsaeng, V. V. (1998).
793 Genetic structure in wild populations of black tiger shrimp (*Penaeus monodon*) using
794 randomly amplified polymorphic DNA analysis. *J Mar Biotechnol*, 6(4), 249-254.
- 795 Tassanakajon, A., Pongsomboon, S., Rimphanitchayakit, V., Jarayabhand, P., & Boonsaeng, V.
796 (1997). Random amplified polymorphic DNA (RAPD) markers for determination of genetic

- 797 variation in wild populations of the black tiger prawn (*Penaeus monodon*) in Thailand. *Mol*
798 *Mar Biol Biotechnol*, 6(2), 110-115.
- 799 Thornber, K., Verner-Jeffreys, D., Hinchliffe, S., Rahman, M. M., Bass, D., & Tyler, C. R. (2019).
800 Evaluating antimicrobial resistance in the global shrimp industry. *Reviews in Aquaculture*, 1-
801 21. doi:10.1111/raq.12367
- 802 Toledo, T. M., Silva, B. C., Vieira, F. d. N., Mourão, J. L. P., & Seiffert, W. Q. (2016). Effects of
803 different dietary lipid levels and fatty acids profile in the culture of white shrimp *Litopenaeus*
804 *vannamei* (Boone) in biofloc technology: water quality, biofloc composition, growth and
805 health. *Aquac Res*, 47(6), 1841-1851. doi:10.1111/are.12642
- 806 Tong, J., Lehnert, S. A., Byrne, K., Kwan, H. S., & Chu, K. H. (2002). Development of polymorphic
807 EST markers in *Penaeus monodon*: applications in penaeid genetics. *Aquaculture*, 208(1-2),
808 69-79. doi:10.1016/S0044-8486(01)00706-2
- 809 Tørresen, O. K., Star, B., Mier, P., Andrade-Navarro, M. A., Bateman, A., Jarnot, P., . . . Linke, D.
810 (2019). Tandem repeats lead to sequence assembly errors and impose multi-level challenges
811 for genome and protein databases. *Nucleic Acids Research*, 47(21), 10994-11006.
812 doi:10.1093/nar/gkz841
- 813 Turkmen, S., Perera, E., Zamorano, M. J., Simó-Mirabet, P., Xu, H., Pérez-Sánchez, J., & Izquierdo,
814 M. (2019). Effects of dietary lipid composition and fatty acid desaturase 2 expression in
815 broodstock gilthead sea bream on lipid metabolism-related genes and methylation of the *fads2*
816 gene promoter in their Offspring. *International Journal of Molecular Sciences*, 20(24), 6250.
817 doi:10.3390/ijms20246250
- 818 Uengwetwanit, T., Ponza, P., Sangsrakru, D., Wichadakul, D., Ingsriswang, S., Leelatanawit, R., . . .
819 Karoonuthaisiri, N. (2018). Transcriptome-based discovery of pathways and genes related to
820 reproduction of the black tiger shrimp (*Penaeus monodon*). *Marine Genomics*, 37, 69-73.
821 doi:10.1016/j.margen.2017.08.007
- 822 Watts, J. L., & Browse, J. (2006). Dietary manipulation implicates lipid signaling in the regulation of
823 germ cell maintenance in *C. elegans*. *Developmental Biology*, 292(2), 381-392.
824 doi:10.1016/j.ydbio.2006.01.013
- 825 Wilson, K., Cahill, V., Ballment, E., & Benzie, J. (2000). The complete sequence of the mitochondrial
826 genome of the crustacean *Penaeus monodon*: Are malacostracan crustaceans more closely
827 related to Insects than to branchiopods? *Molecular Biology and Evolution*, 17(6), 863-874.
828 doi:10.1093/oxfordjournals.molbev.a026366
- 829 Wilson, K., Li, Y., Whan, V., Lehnert, S., Byrne, K., Moore, S., . . . Benzie, J. (2002). Genetic
830 mapping of the black tiger shrimp *Penaeus monodon* with amplified fragment length
831 polymorphism. *Aquaculture*, 204(3-4), 297-309. doi:10.1016/S0044-8486(01)00842-0
- 832 Wongsurawat, T., Leelatanawit, R., Thamniemdee, N., Uawisetwathan, U., Karoonuthaisiri, N.,
833 Menasveta, P., & Klinbunga, S. (2010). Identification of testis-relevant genes using in silico
834 analysis from testis ESTs and cDNA microarray in the black tiger shrimp (*Penaeus monodon*).
835 *BMC Molecular Biology*, 11, 55. doi:10.1186/1471-2199-11-55
- 836 Wu, T. D., & Watanabe, C. K. (2005). GMAP: a genomic mapping and alignment program for mRNA
837 and EST sequences. *Bioinformatics*, 21(9), 1859-1875. doi:10.1093/bioinformatics/bti310
- 838 Wuthisuthimethavee, S., Aoki, T., Hirono, I., & Tassanakajon, A. (2009). Preliminary study of BAC
839 library construction in black tiger shrimp, *Penaeus monodon*. *Walailak Journal of Science and*
840 *Technology*, 6(1), 37-48.
- 841 Yu, Y., Zhang, X., Yuan, J., Li, F., Chen, X., Zhao, Y., . . . Xiang, J. (2015). Genome survey and high-
842 density genetic map construction provide genomic and genetic resources for the Pacific White
843 Shrimp *Litopenaeus vannamei*. *Scientific Reports*, 5(1), 15612. doi:10.1038/srep15612
- 844 Yuan, J., Zhang, X., Liu, C., Yu, Y., Wei, J., Li, F., & Xiang, J. (2018). Genomic resources and
845 comparative analyses of two economical penaeid shrimp species, *Marsupenaeus japonicus*
846 and *Penaeus monodon*. *Marine Genomics*, 39, 22-25. doi:10.1016/j.margen.2017.12.006

- 847 Zhang, X., Yuan, J., Sun, Y., Li, S., Gao, Y., Yu, Y., . . . Xiang, J. (2019). Penaeid shrimp genome
848 provides insights into benthic adaptation and frequent molting. *Nat Commun*, 10(1), 356.
849 doi:10.1038/s41467-018-08197-4
- 850 Zhao, C., Zhang, X., Liu, C., Huan, P., Li, F., Xiang, J., & Huang, C. (2012). BAC end sequencing of
851 Pacific white shrimp *Litopenaeus vannamei*: a glimpse into the genome of Penaeid shrimp.
852 *Chinese Journal of Oceanology and Limnology*, 30(3), 456-470. doi:10.1007/s00343-012-
853 1159-y

854
855 **Data accessibility**

856 The genomic and transcriptomic data are available in the NCBI under the following accession
857 numbers: PRJNA611030 and PRJNA602748. The annotation file and genome sequences are available
858 from the following website: <http://www.biotech.or.th/pmonodon/index.php>.

859

860 **Author contributions**

861 PA, KS, SA, RL and JK collected samples. PA, KS, SA, TW, RL, DS extracted DNA and RNA
862 for sequencing. TU, WP, and CS carried out genome assembly and assessment. TU, JK, PS and VS
863 were responsible for the gene prediction and annotation. TU, WP, and CS performed repeat analysis.
864 IN and PJ carried out comparative genome analysis. TU, SA, WR and NK performed differential
865 expression analysis and validation. WP, IN, FT and NK supervised this project. TU, WP, IN, and NK
866 wrote the manuscript. All authors contributed to the final manuscript editing.

867

868

869

870

871

872

873

874

875

876 **Table**

877 **Table 1. Assembly statistics of the *P. monodon* genome.**

	PacBio	PacBio+Chicago	PacBio+Chicago +Hi-C
Number of contigs/scaffolds	70,380	30,179	26,877
Number of contigs/scaffolds > 1 kb	70,373	30,171	26,869
Number of contigs/scaffolds > 50 kb	11,084	3,725	869
Number of contigs/scaffolds > 1 Mb	6	569	44
Number of contigs/scaffolds > 10 Mb	-	1	43
Total length (bases)	2,389,954,102	2,394,031,700	2,394,363,600
Longest contig/scaffold (bases)	1,387,722	12,098,070	65,869,259
Mean contig/scaffold size (bases)	33,958	79,328	89,086
Contig/scaffold N50 (Mb)	0.079	1.157	44.862
Contig/scaffold L50	6,786	509	23
% N in scaffolds	-	0.17	0.18
Genome annotation			
		Number of genes	31,641
		Number of transcripts	36,538
		Average gene length (bp)	1,428
		Number of annotated genes:	
		Refseq	30,038
		Uniprot	10,068
		GO	22,243
		InterPro	20,615

878

879

880 **Figure Legends**

881 **Figure 1. *P. monodon* genome assembly and phylogenetic analysis.**
882 (A) Genomic landscape of 44 assembled *P. monodon* chromosomes. (a) Physical map of *P.*
883 *monodon* chromosomes (Mb scale). (b) Density of repetitive sequences represented by percentage of
884 genomic regions covered by simple repeat sequences in 500-kb window. (c) Gene density represented
885 by number of genes in 500-kb window. (d) GC content represented by percentage of G/C bases in 500-
886 kb window. Syntenic blocks are depicted by connected lines. (e) Syntenic relationship of gene blocks
887 among *P. monodon* chromosomes. Syntenic blocks were identified by MCScanX with criteria at least
888 ten syntenic genes and a maximum of six intervening genes allowed. (B) Diagrams
889 showing colinearity between *P. monodon* and *L. vannamei* chromosomes. Lines link the position of
890 orthologous gene sets. Most regions exhibit one-to-one relationship between *P. monodon* and *L.*
891 *vannamei*. The yellow line represents the region on a single *P. monodon* chromosome that exhibits
892 synteny to regions on two *L. vannamei* chromosomes. Black tiger shrimp chromosomes are designated
893 with “P” followed by chromosome numbers, and Pacific white shrimp chromosomes are designated
894 with “L” followed by the chromosome numbers. (C) Diagrams showing colinearity between *P.*
895 *monodon* and *L. vannamei* where the syntenic relationship between chromosomes is not one-to-one.
896 (D) Phylogenetic tree of concatenated mitochondria protein-coding genes using maximum likelihood
897 general reversible mitochondrial model. The percentage of trees in which the associated taxa clustered
898 together is shown next to the branches. The tree is drawn to scale, with branch lengths measured in the
899 number of substitutions per site.

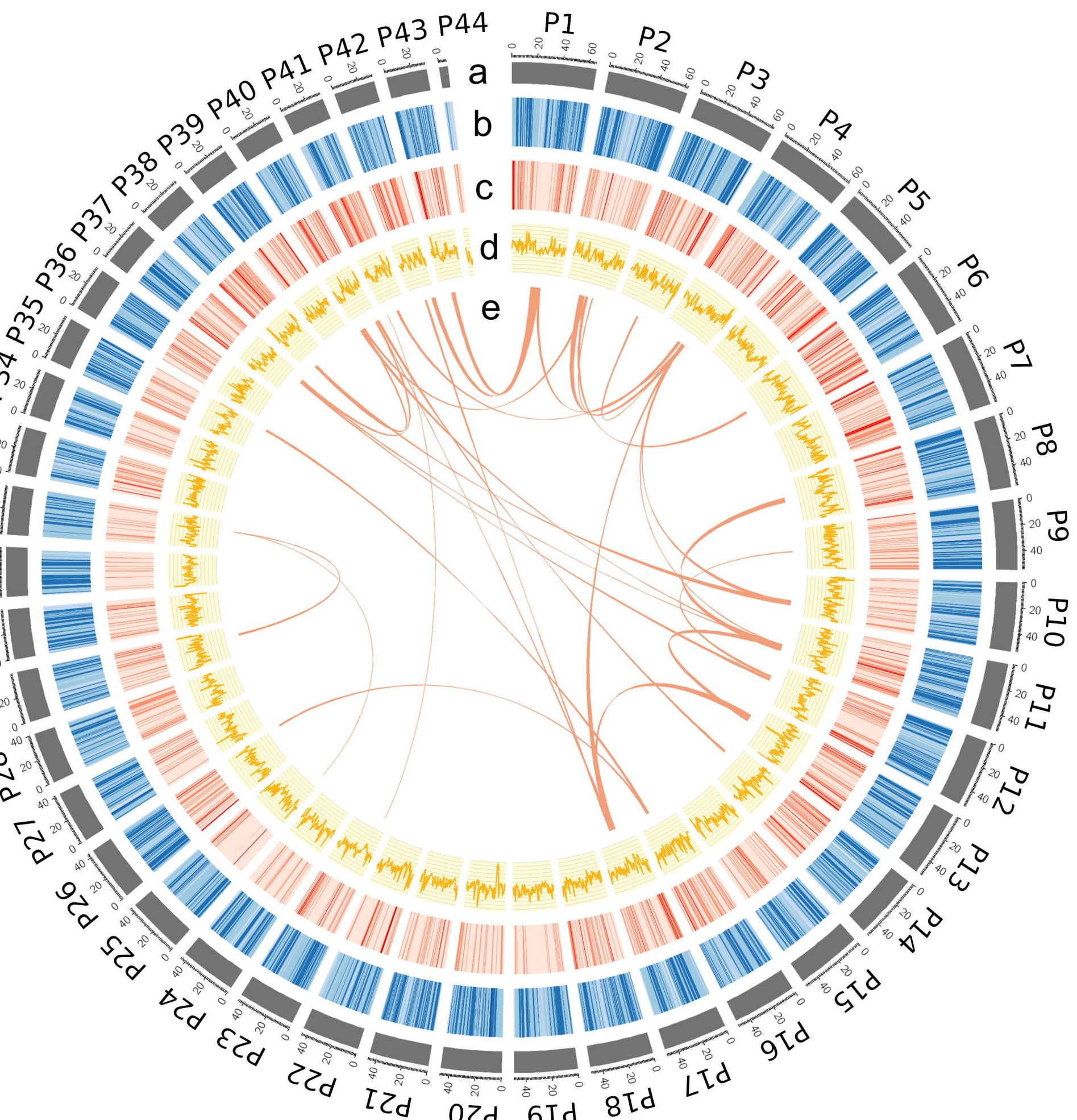
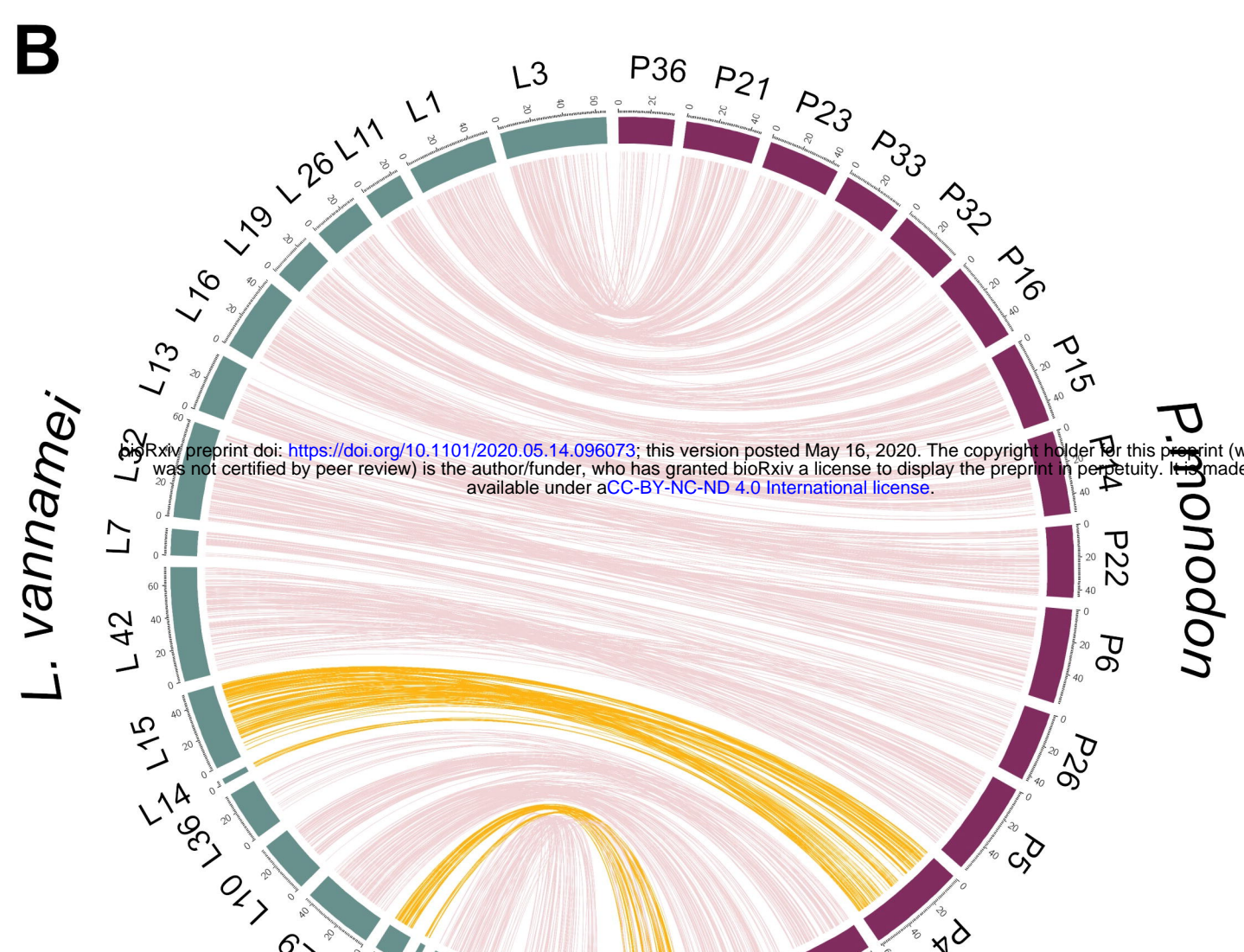
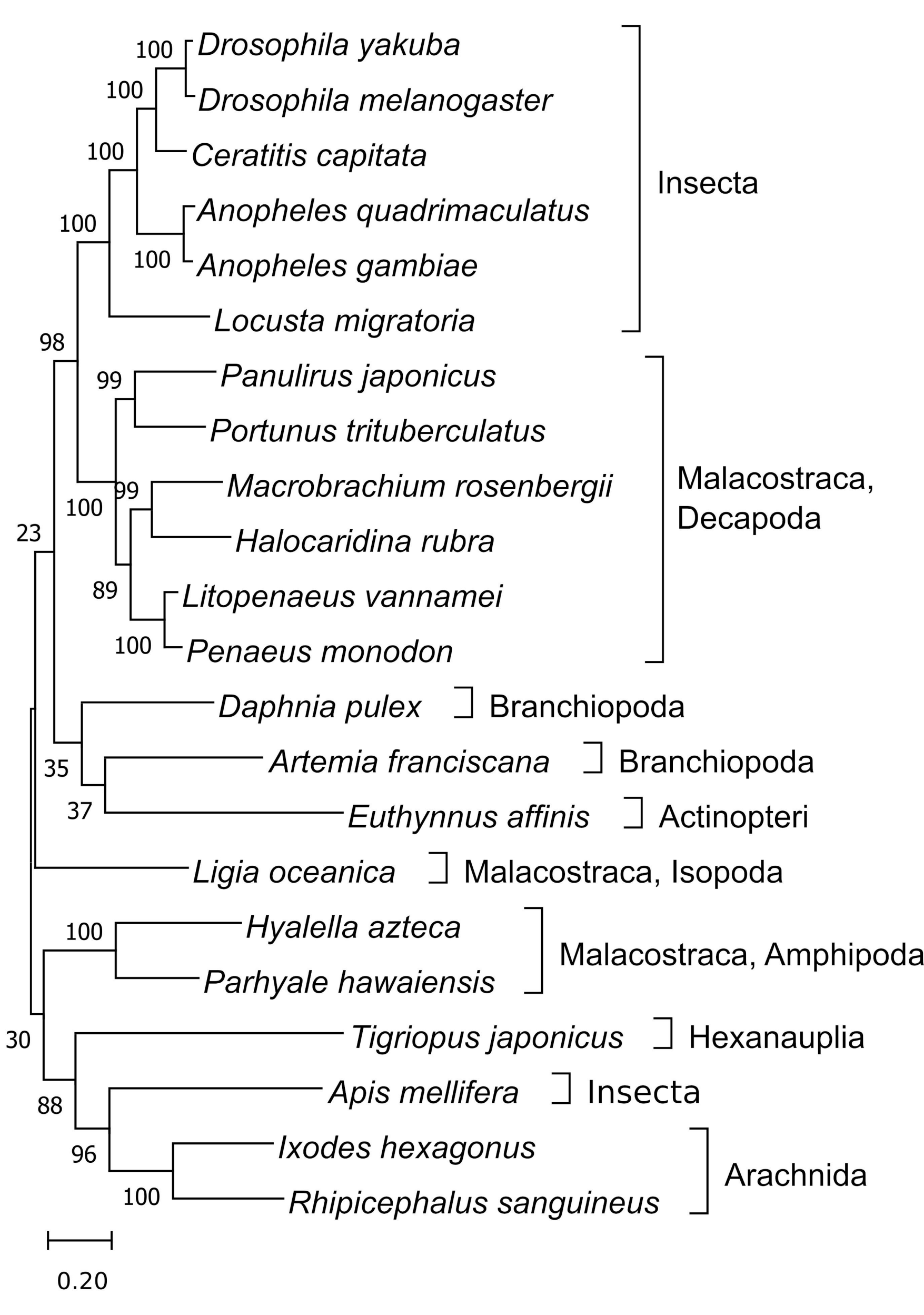
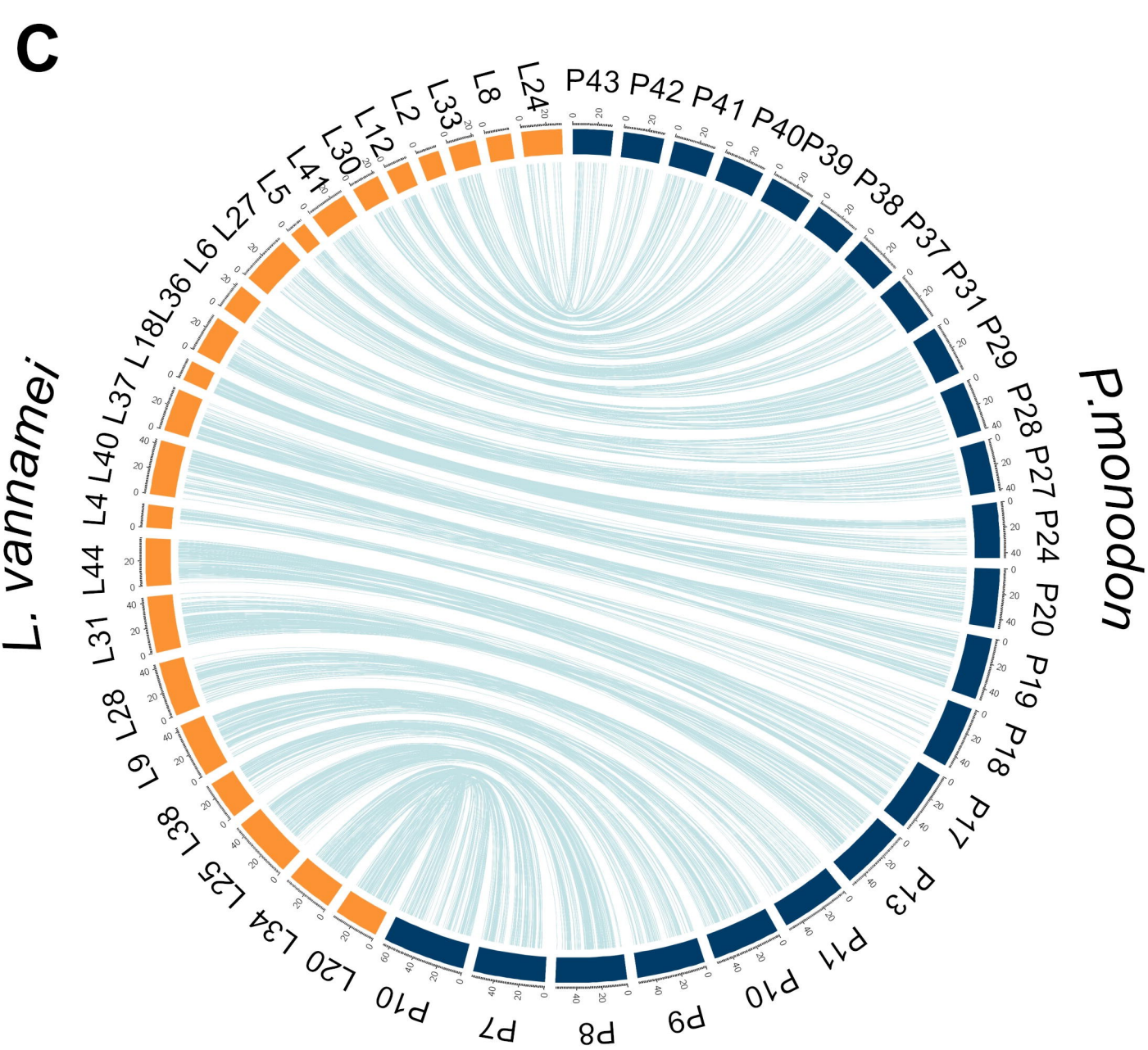
900

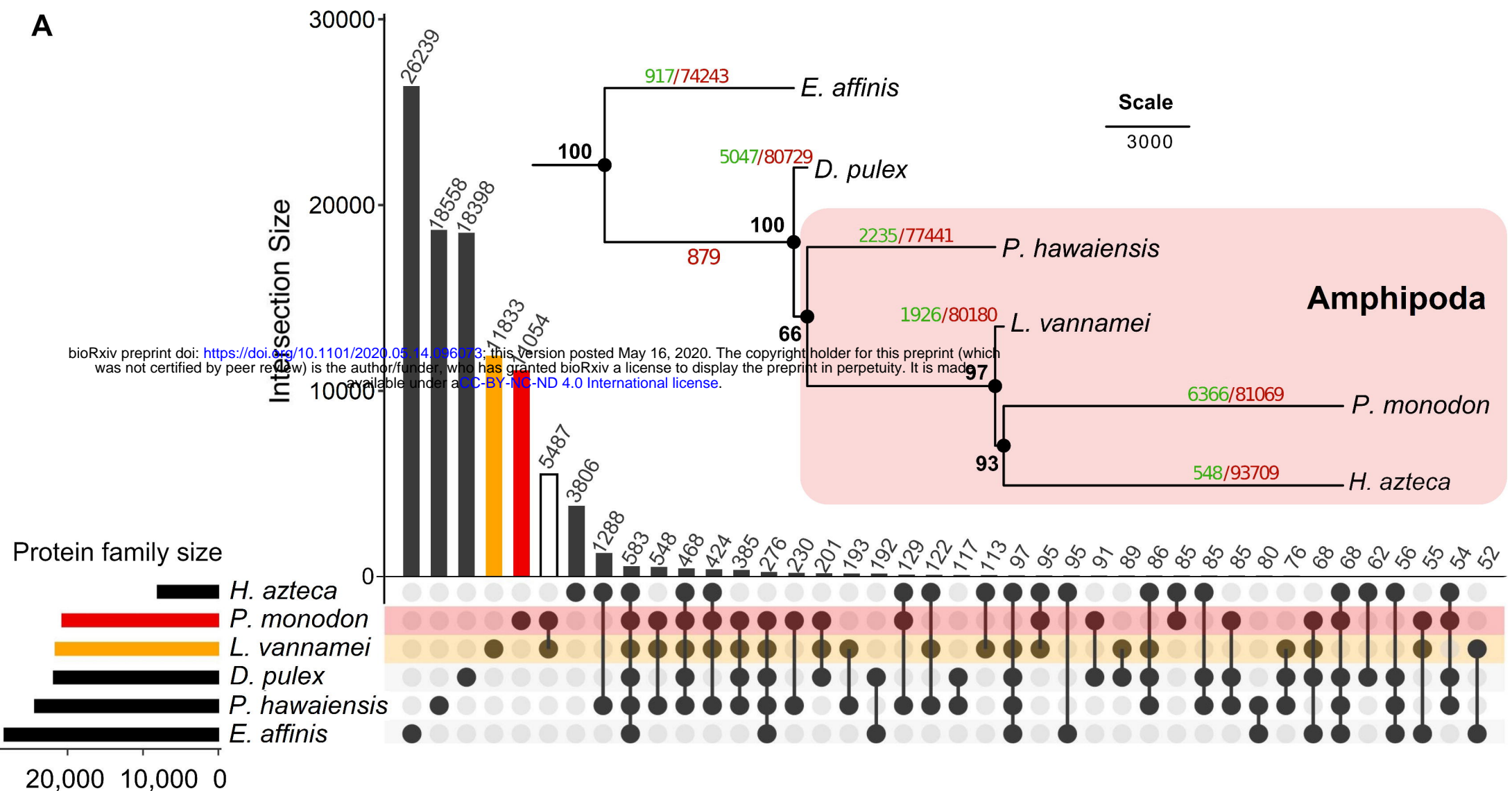
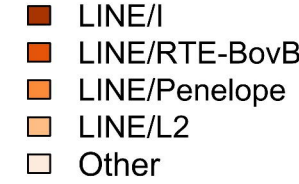
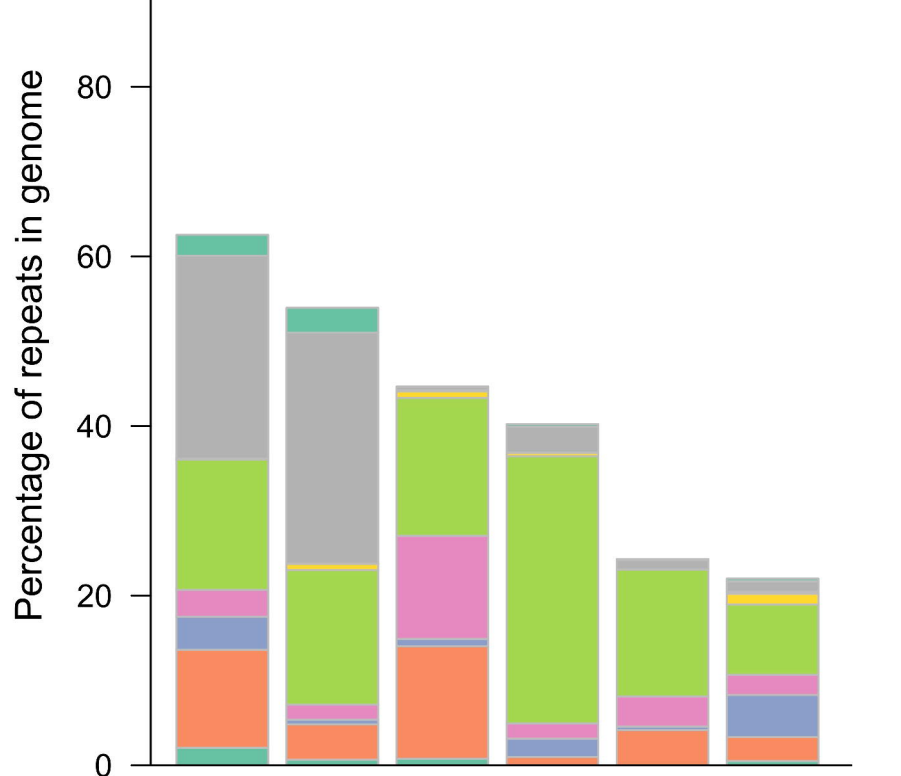
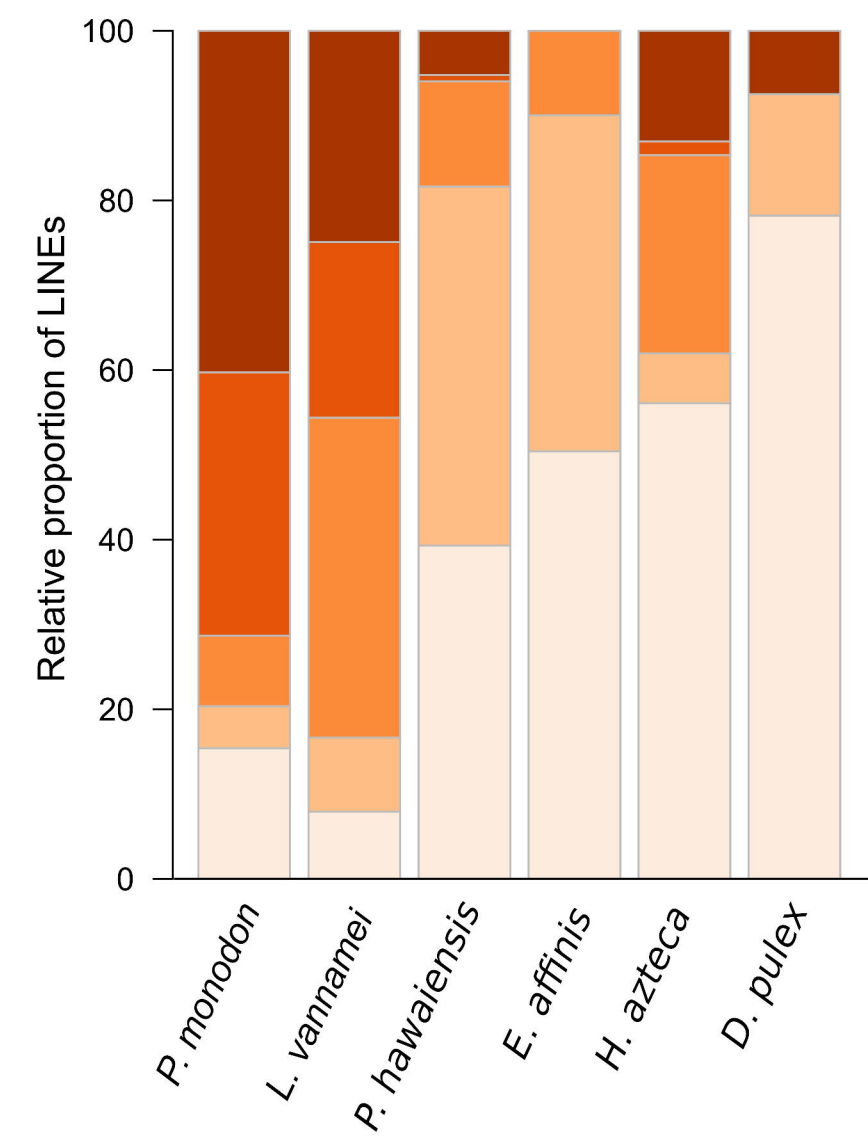
901 **Figure 2. Comparative genomics and repeat elements analysis.**

902 (A) Upset plot represents pan-core protein family of crustacean genomes (*P. monodon*, *L. vannamei*,
903 *P. hawaiensis*, *E. affinis*, *H. azteca*, and *D. pulex*) with the pan protein family tree with bootstrap value
904 in black numbers. The numbers on branches indicate the number of protein family gains (green) or
905 losses (red). Relative proportion or repeat elements in the crustacean genomes is presented as (B) bar
906 plots of percentage of repeat elements and (C) relative abundance of each LINE type.
907

908 **Figure 3. Expression of differentially expressed genes of slow-growing shrimp (n=15) and fast-**
909 **growing shrimp (n=15).**

910 (A) The top five enriched COGs metabolism groups were carbohydrate transport and metabolism,
911 secondary metabolites biosynthesis, transport and catabolism, inorganic ion transport and metabolism,
912 lipid transport and metabolism and amino acid transport and metabolism. (B) Differentially expressed
913 genes in PI3K-Akt pathway. Blue letters indicate newly identified genes in *P. monodon*, and the
914 dagger (†) indicates genes that were further validated by quantitative real-time PCR.
915

A**B****D****C**

A**B****C****B****C**

A

Slow-growing shrimps (n=15)	Fast-growing shrimps (n=15)	Log ₂ FC	Description	
		2.45	mannan endo-1,4-beta-mannosidase-like	
		2.44	venom carboxylesterase-6-like	
		1.74	alpha-amylase-like isoform X1	
		1.71	serine/threonine-protein phosphatase CPPED1-like	
		1.56	fructose-bisphosphate aldolase isoform X1	
		1.50	cholinesterase 1-like	
		1.46	beta-1,4-glucuronidyltransferase 1-like	
		1.38	venom carboxylesterase-6-like	
		1.32	chitooligosaccharidolytic beta-N-acetylglucosaminidase-like	
		1.32	venom carboxylesterase-6-like	
		1.31	cholinesterase 1-like	
		1.28	putative inorganic phosphate cotransporter isoform X2	
		1.21	alpha-mannosidase 2C1	
		1.11	+ insulin-like growth factor 1 receptor	
		1.06	spingomyelin phosphodiesterase-like	
		1.04	UDP-glucuronosyltransferase 2B14-like	
		1.02	alpha-N-acetylgalactosaminidase	
		1.01	glucose-6-phosphate exchanger SLC37A2-like	
		1.01	glyceraldehyde-3-phosphate dehydrogenase 2-like	
		-1.14	xylosyltransferase oxt	
		-1.17	putative inorganic phosphate cotransporter	
		-1.59	cholinesterase 2-like isoform X1	
		2.40	+ nos resistant to fluoxetine protein 6-like	
		1.72	+ glycerol-3-phosphate acyltransferase 3 isoform X2	
		1.54	acyl-CoA Delta(11) desaturase-like	
		1.43	fatty acid hydroxylase domain-containing protein 2 isoform X1	
		1.42	lipase member H	
		1.29	putative acyl-coenzyme A oxidase 3.2, peroxisomal	
		1.27	G-protein coupled receptor Mth2-like	
		1.27	pancreatic lipase-related protein 2-like	
		1.22	cellular retinoic acid-binding protein 1-like	
		1.17	long-chain-fatty-acid-CoA ligase 4 isoform X1	
		1.10	non-specific lipid-transfer protein	
		1.06	sodium/calcium exchanger regulatory protein 1-like	
		1.03	lipase 3-like	
		-1.04	AMP-binding protein	
		-1.11	beta-1,3-glucan-binding protein precursor	
		-1.22	4-coumarate-CoA ligase 1-like	
		-1.60	+ elongation of very long chain fatty acids protein 4-like	
		-2.08	apolipoporphins-like	
		2.10	xaa-Pro aminopeptidase 1-like	
		1.62	RNA-directed DNA polymerase from mobile element jockey-like	
		1.38	cystathione beta-synthase-like isoform X1	
		1.29	N-fatty-acyl-amino acid synthase/hydrolase PM20D1	
		1.28	arginase-2, mitochondrial	
		1.20	+ phospholipid phosphatase 2-like	
		1.15	agmatinase, mitochondrial	
		1.11	phenoloxidase 2	
		1.02	kyurenimine formamidase isoform X1	
		-1.06	phosphoserine phosphatase isoform X2	
		-1.17	methionine synthase-like	
		-1.48	betaine-homocysteine S-methyltransferase 1-like	
		-1.71	Y+L amino acid transporter 2	
		2.24	laccase-4 isoform X2	
		1.94	cytochrome P450 9e2-like isoform X3	
		1.82	cytochrome P450 2L1-like	
		1.44	sorbitol dehydrogenase	
		1.35	estradiol 17-beta-dehydrogenase 8-like	
		1.33	cytochrome P450 3A24-like isoform X3	
		1.25	multidrug resistance-associated protein 1 isoform X4	
		1.19	probable cytochrome P450 49a1	
		1.14	estradiol 17-beta-dehydrogenase 8	
		1.12	guanine deaminase-like	
		1.11	short-chain dehydrogenase/reductase family 16C member 6-like	
		1.10	probable cytochrome P450 49a1	
		1.07	cytochrome P450 2B4-like	
		-1.07	ATP-binding cassette sub-family B member 8, mitochondrial-like	
		-1.55	retinol dehydrogenase 13-like	
		2.93	+ transferrin-like	
		1.85	bestrophin homolog 17-like isoform X1	
		1.64	zinc transporter ZIP1-like	
		1.59	sodium/hydrogen exchanger 7 isoform X5	
		1.20	soma ferritin-like	
		1.18	innexin inx2	
		1.14	innexin inx2-like	
		1.13	facilitated trehalose transporter Tret1-like	
		1.09	sodium-dependent phosphate transporter 2	
		1.04	innexin shaking-B-like	
		1.02	probable glutamate receptor	
		-1.19	+ sodium/hydrogen exchanger 2 isoform X1	
		-1.63	excitatory amino acid transporter 1-like	
		-2.04	prestin-like isoform X2	



Carbohydrate transport and metabolism

Lipid transport and metabolism

Amino acid transport and metabolism

Secondary metabolites biosynthesis, transport and catabolism

Inorganic ion transport and metabolism

B

Slow-growing shrimps (n=15)	Fast-growing shrimps (n=15)	Log ₂ FC	Description	
		1.64	+ serine/threonine-protein kinase N isoform X1	
		1.53	+ integrin alpha-4-like	
		1.11	+ insulin-like growth factor 1 receptor	
		1.11	integrin beta-PS isoform X1	

P13K-Akt signaling